Nigerian Journal of Physics (NJP)
ISSN online: 3027-0936
ISSN print: 1595-0611
DOI: https://doi.org/10.62292/njp.v34i2.2025.366
Volume 34(2), June 2025

Application of Transition Metal Dichalcogenides in Electrocatalytic Splitting of Water for Hydrogen Production: A Review

*[1]Shamsuddeen, S. A., Abdulsalam, M. and Tanimu, A.

Department of Physics, Umaru Musa Yar'adua University, Katsina, Katsina State, Nigeria.

*Corresponding author's email: shamsuddeen.sani@umyu.edu.ng

KEYWORDS:
Carbon Emissions,
Electrocatalysts,
Fossil fuels,
Green Hydrogen,
Transition Metal Dichalcogenides.

ABSTRACT

The world aims to reduce carbon emissions by transition to alternative and renewable energy sources such as green hydrogen, which is cleaner and more sustainable for various applications compares to the traditional fossil fuels. Electrocatalytic splitting of water is one of the best promising method for hydrogen production due to its affordability, sustainability, and eco-friendliness. Transition metal dichalcogenides (TMDs) have emerged as the essential electrocatalysts for this process. This paper presents a review on the progress in TMDs as electrocatalysts. It starts with a concise discussion on the overview of TMDs and their unique properties that made them attractive in the electrocatalysis of water. However, various descriptors of a good electrocatalyst were elaborated as well as some of the ways of improving the catalytic activity of the existing TMDs-based electrocatalysts. The methods of synthesis of the TMDs-based electrocatalysts were also explored. The paper concludes by pointing out some of the challenges that hinder the progress of the field and future directions that will greatly contribute toward improving the entire field of electrocatalytic splitting of water for effective hydrogen generation.

INTRODUCTION

It is evidently clear that, the world is in the quest of achieving zero carbon emissions, as such, the ever pressing need to eliminate burning fossil fuels has becomes necessary (Sukanya et al., 2022). Because burning fossil fuels releases carbon dioxide (CO_2) which is one of the greenhouse gases that are very detrimental to the human health, plants and environment among others (Zhao et al., 2017; Hoegh-Guldberg et al.,2007; Polvani et al., 2020). Therefore, transition to renewable and alternative energy sources that are affordable, sustainable and environmentally friendly will greatly solve the problem. To this regard, hydrogen is regarded as a clean fuel that can replace the use of traditional fossil fuels in homes, vehicles, industries etc. (Turner, 2004; Jiao et al., 2015; Guo et al., 2019; Dresselhaus and Thomas, 2001; Zhang et al., 2016; Zhou et al., 2019).

However, there are various methods of hydrogen production, but some of them are very expensive and even lead to the emission of CO_2. For example, the popularly known steam reforming process of hydrogen generation (in industry) causes environmental pollution (Fu et al., 2020). In contrast, electrocatalytic splitting of water is considered as one of the most promising approaches in the production of hydrogen due to its affordability, sustainability and environmentally friendly nature (Zhu et al., 2020; Dresp et al,. 2019). This method isn't achievable without electrocatalysts. They are highly required in order to speed up the kinetics of the hydrogen evolution reaction (HER) and reduce the electrical energy consumption of the process (Fu et al., 2020). The widely use electrocatalysts are platinum (Pt), Iridium (Ir) and some other precious-metal-based compounds, only that those materials are very scarce and expensive, as such their applications are restricted (Faber and Jin, 2014; Ding et al., 2016; Yin et al., 2016; Wang et al., 2017; Li et al., 2019; Liang et al., 2019). Hence there is a need to develop new electrocatalysts that are cheaper and abundant but with excellent properties comparable to the precious Pt-groups. Researchers have recently focused on the transition metals based electrocatalysts such as transition metal dichalcogenides (TMDs), hydroxides, carbides, borides, nitrides, and phosphides, and even metal-free carbon-based materials, such as graphene and carbon nanotubes (Wazir et al., 2022; Fu et al., 2022; Gholamvand et al., 2016; Najafi et al., 2018; Henckel et al., 2018).

Among all the aforementioned non-precious materials, TMDs were reported to be the best substitutes for the Pt-groups due to their unique and interesting properties (Li et al., 2018; Sukanya et al., 2022). Some of those properties that made them most attractive are their layered structures, tunable band gaps, outstanding chemical stability, high catalytic activities, earth-abundant and low-cost. Specifically, the TMDs that gained more attentions are the two-dimensional (2D) TMDs, such as molybdenum diselenide ($MoSe_2$), molybdenum disulfide (MoS_2), tungsten diselenide (WSe_2), and tungsten disulfide (WS_2), (Gholamvand et al., 2016; Najafi et al., 2018; Henckel et al., 2018; Li et al., 2018; Lin et al., 2014; Yang et al., 2015; Li et al., 2019).

Moreover, it is obvious that there are many excellent previous reviews that focus on the use of TMDs-based electrocatalysts for hydrogen generation (Fu et al., 2020; Sukanya et al., 2022; Sim et al., 2022; Zeng et al, 2024). Still much work is required to fully understand and utilize those materials for efficient and scalable hydrogen production. Thus, herein we systematically reviewed the application of the TMDs in electrocatalytic splitting of water and particularly emphasized on the need to employ hybrid approach within the framework of density functional theory (DFT) and machine learning in the discovery and preparation of novel TMDs-based electrocatalysts. We started with the overview of the transition metal chalcogenides, and subsequently delved into the TMDs. The properties that made the TMDs to be more attractive electrocatalysts were reviewed. The concept of electrocatalysis was also highlighted with more emphasis on the hydrogen and oxygen evolution reactions. Not only that, we also discussed the descriptors of good electrocatalysts. The methods of synthesis of the TMDs-based electrocatalysts were also explored. Finally, the challenges and future directions were discussed with the sole intention of exploring more TMDs based electrocatalysts for effective hydrogen generation.

Overview of Transition Metals Chalcogenides (TMCs)

The transition metals chalcogenides (TMCs) are chemical compounds that consist of two parts; the transition metals and chalcogen elements. They have a general formula MX_n, where M = transition metals such as molybdenum (Mo), tungsten (W), vanadium (V), rhenium (Re), thallium (Ta), titanium (Ti), X = chalcogens either sulfur (S), selenium (Se), or tellurium (Te) and subscript n = the atomicity of the chalcogen and it can take values 1, 2, 3. There is quite a number of possible layered structure materials consist of sixteen (16) transition metals and three (3) chalcogens atoms (Han et al., 2015) as shown in figure 1. However, there are three classes of TMCs depending on the atomicity (n) of the chalcogen atoms (Kheibar et al., 2023). They are:

i. Transition metal monochalcogenides (TMMs) when n = 1, with the general formula MX (M = Cu, Ag; X = S, Se or Te).
ii. Transition metal dichalcogenides (TMDs) when n = 2, with the general formula MX_2 (M = W, Mo as semiconductor and V, Nb, Ta as metal; X = S, Se or Te).
iii. Transition metal trichalcogenides (TMTs) when n = 3, with the general formula MX_3 (M = Ti, Zr, Hf, V, Nb, Ta, Db and Cr; X = S, Se or Te) and this is the less studied family.

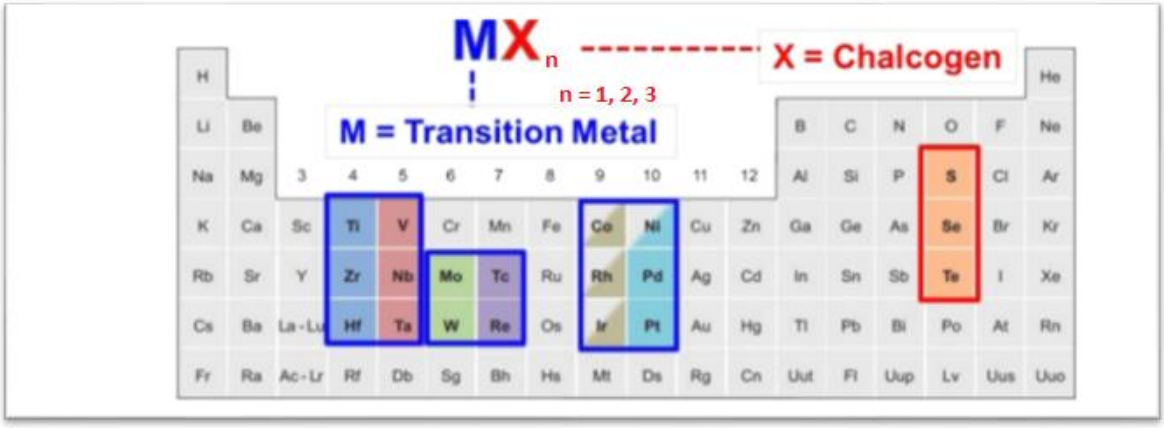

Figure 1: The periodic table showing 16 transition metals and 3 chalcogen atoms obtained from (Han et al., 2015; Chhowalla et al., 2013)

Transition Metals Dichalcogenides (TMDs)

After the discovery of graphene, a lot of new two-dimensional (2D) materials were reported (Sun et al., 2022; Yu and Breslin, 2020; Sukanya et al.,2022; Manzeli et al., 2017), among which are transition metal dichalcogenides (TMDs) with the chemical formula MX_2 (M = W, Mo as semiconductor and V, Nb, Ta as metal; X = S, Se or Te). This class of materials has gained much

attention around the globe due to their unique and fascinating properties that include but not limited to high surface areas, good chemical stability and tunable band gaps (Sun et al., 2022).

Structural Properties of TMDs

The interesting and outstanding properties of TMDs are highly connected to their crystal and electronic structures (Liu et al., 2017; Mak et al., 2010; Splendiani et al., 2010; Wilson et al., 1974). The TMDs exhibit a layered structure similar to that of graphite, with each single layer composed of stacked X−M−X sheets and the sequential stacking of layers forming the material. Each layer is weakly coupled by the van der Waals force, whereas the metal−chalcogen bond is covalent in nature (Giuffredi et al., 2021). However, according to the nature of the metal and chalcogen atoms, the stacking of the various X−M−X layers and the metal coordination in each layer may vary, giving rise to different polymorphs. The TMDs can exhibit different phases, with the two main heterogeneous polymorphic structures being the octahedral coordination phase (1T) as shown in figure 2(B), which shows metallic-like properties, and the trigonal prismatic phase (2H), which gives semiconductor-like properties as illustrated in figure 2(A). However, in the H phase for the hexagonal symmetry (Figure 2A), the six X atoms are arranged symmetrically in the upper and lower tetrahedrons with the KKK M atoms as the symmetrical point. The 2H and 3R phases are identified based on sequence stacking of the 1H layer. The two layers with AB stacking as a unit cell in the 2H phase show a hexagonal symmetry (point group D_{3h}), whereas the 3R phase composed of three layers with ABC stacking exhibits a rhombohedral symmetry (point group C_{3v}). Another major structure, the T phase shown in Figure 2B, is formed by rotating the upper (or lower) tetrahedron by 180^0, which characterizes tetragonal symmetry (point group D_{3d}). Furthermore, the dimerization of transition metal atoms can lead to the distortion of the 1T phase including the monoclinic (1T') and orthorhombic (T_d) structures (Sim et al., 2022).

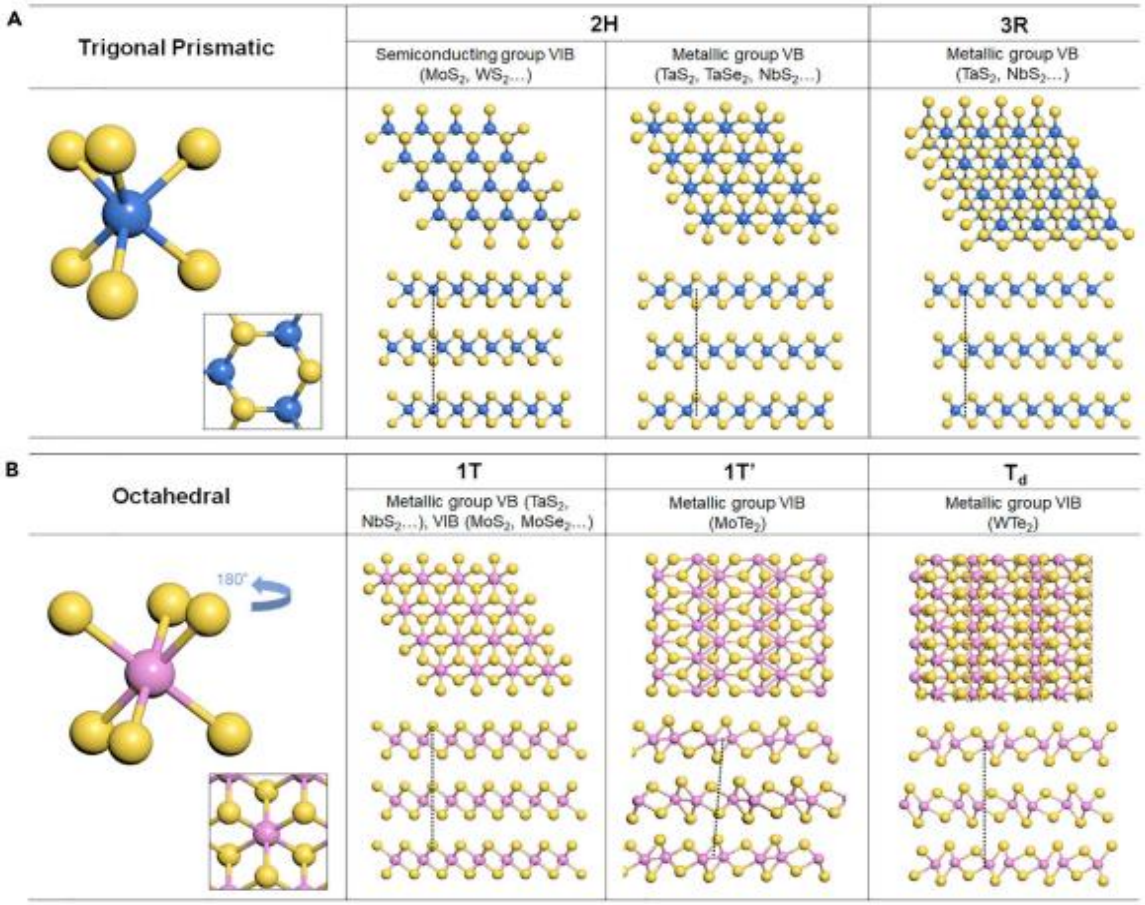

Figure 2: Crystal Structure of TMDs (A) H-Phases (B) T- Phases obtained from (Sim et al., 2022). In this notation, the digit signifies the number of X−M−X layers in the crystalline unit cell, and the letter gives the symmetry of the material: T refers to a tetragonal symmetry, H to hexagonal symmetry, and R for rhombohedral symmetry

Furthermore, the 1T phase is characterized by having a low charge transfer resistance and enhanced electrocatalytic activity, thereby making it a very interesting material for electrochemical applications (Tang and Jiang, 2016). On the other hand, the 2H phase is the most favourable phase thermodynamically. However, solution phase intercalation is one of the popular methods used in the conversion of the 2H to 1T polymorph. Also, it was reported that non-metal doping with phosphorus (P) can be used to promote the formation of the metallic 1T phase (Sun et al., 2022).

The creation of defects and distortions to give active sites on the TMDs layered structures has become an intense research topic in recent years with various transition metals doped TMDs emerging (Xiong et al., 2018;Kunhiraman et al., 2021;Huang et al., 2021). Methods such as defect engineering, electron beam irradiation or heteroatom doping (Ye et al., 2016; Ramki, et al., 2019) can be employed to give a high density of active sites.

Electronic Properties of TMDs

The tunability of electronic band gap of TMDs is one of the factors that made them more attractive and applicable in so many areas. For example, Coehoorn et al., claimed that some of the TMDs have band gaps that matched solar spectrum (Coehoorn et al., 1987). This made them very good candidates for photocatalytic water splitting. However, the decrease in the thickness of the layers of the TMDs has a significant effect on their band gaps. It was reported that the band gap of MoS_2 increases from 1.29 eV to 1.9 eV as the thickness reduced from bulk to a monolayer (Kam and Parkinson, 1982; Splendiani et al., 2010; Mak et al., 2010). This is as a result of quantum-mechanical confinement in the vertical direction and the resulting change in hybridization in orbitals related to transition metal (M) and chalcogen (X) atoms. However, the bulk MoS_2 material exhibits an indirect band gap behavior whereas the single layer MoS_2 is a direct gap semiconductor. This seems to be a general characteristic exhibited by many other semiconducting TMDs (Kuc et al., 2011; Li and Galli, 2007; Liumet al., 2011; Ding et al., 2011; Ataca et al., 2012)

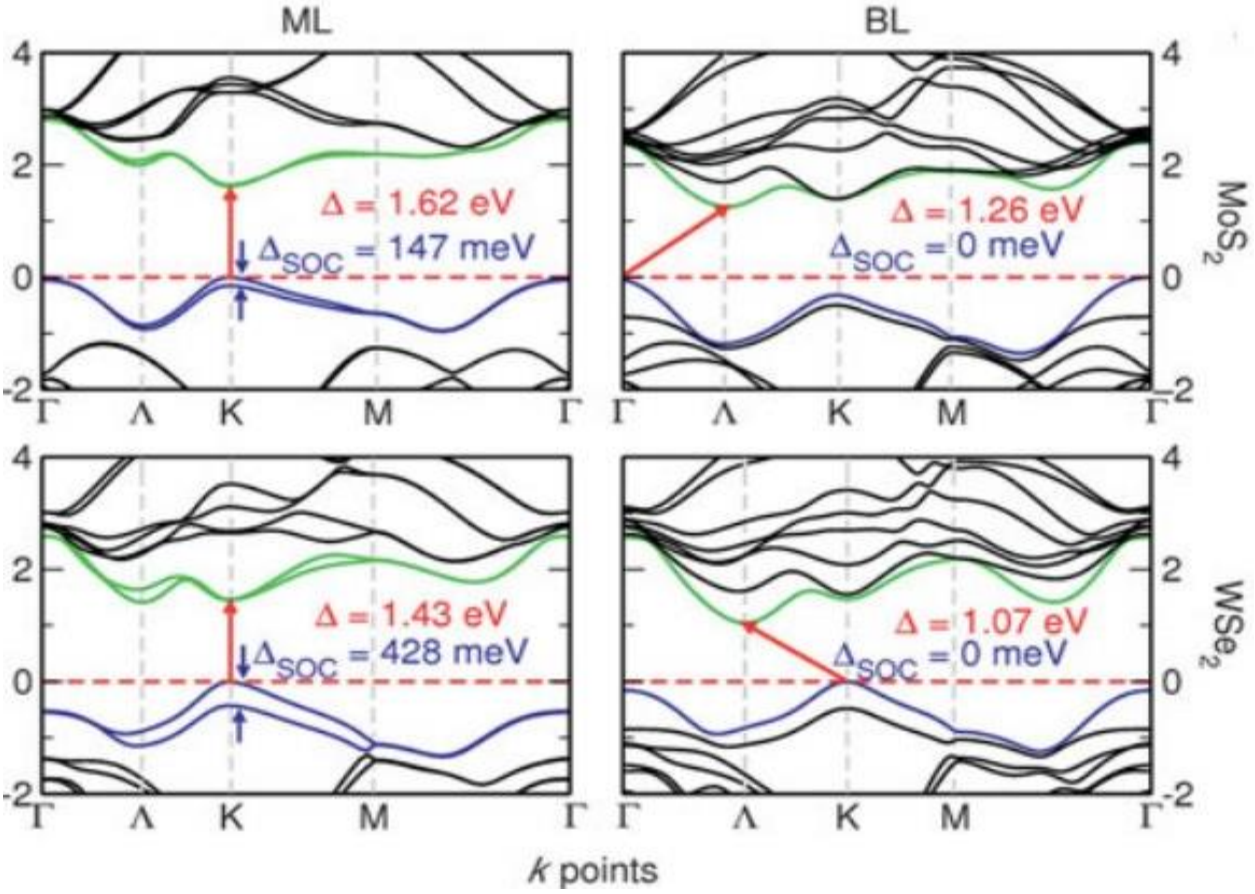

Figure 3: Band structure of MoS_2 (top) and WSe_2 (bottom) for monolayer (ML) and bilayer (BL) obtained from reference (Kuc et al., 2015)

Figure 3 illustrates that the MoS_2 and WSe_2 when thinned down to monolayers, undergo the indirect to direct bandgaps transition (Kuc et al., 2015). However, using calculations based on density functional theory (DFT), Zhu et al. reported massive spin–orbit (SO) splitting for MoS_2 monolayer (Zhu et al., 2011). Because of the interplay between the inherent electron spin and its angular orbital momentum, this powerful quantum effect modifies the material's electronic levels based on their spin signature. With values reaching 480 meV for WTe_2, this effect is likewise universal for all 2H Group VI TMD materials (Zibouche et al.,2014). Giant SO splittings are visible in monolayers, but they are not present in the bulk or in bilayers as depicted in figure 3. This discrepancy can be attributed to the existence of an inversion center, which produces two degenerate orbitals with opposite spin at any given position in the band structure. Hence, it is possible to exploit the symmetry for tuning the SO splitting, offering interesting materials for spintronic applications (Kuc et al., 2015).

However, defects that frequently arise as a result of the synthesis process have a significant impact on the electronic characteristics of TMD materials. For example, in MoS_2 MLs, point defects result in additional photoemission peaks and increased photoluminescence intensity (Tongay et al., 2013). Localized excitons and the trapping capacity of free charge carriers are responsible for these effects. Electronic and structural simulations of faulty MoS_2 ML reveal that defects introduce mid-gap states that serve as scattering centers (Ghorban-Asl et al., 2013).

Electrocatalytic Splitting of Water

Electrocatalytic splitting of water is the process of breaking down water (H_2O) into oxygen (O_2) and hydrogen (H_2) gas with the use of an electric current. It is also known as water electrolysis. However, the whole process of electrocatalytic splitting of water involves two half reactions which take place at different electrodes; the hydrogen evolution reaction (HER) at the cathode and oxygen evolution reaction (OER) at the anode (Fu et al., 2020). A chemical substance called electrocatalyst is needed to speed up the rate of these reactions. The electrocatalysts are very crucial in the process, because in addition to increasing the rate of the reactions, they reduce the electrical consumption of the entire process.

Hydrogen Evolution Reaction (HER)

HER is the reduction of proton (H^+) to form hydrogen gas (H_2). It involves two different mechanisms in electrolyte. These are:

Volmer–Tafel (V–T) Mechanism: This mechanism forms the adsorbed hydrogen atom (H^*_{ads}) at the active site of the catalyst, when a transferred electron first combines with a proton (acidic solution) or water molecule (in basic solution) and is adsorbed by the catalyst (the Volmer step). Then, two H^*_{ads} combine to produce H_2 gas (the Tafel step) as seen in table 1. The hydrogen adsorption site is indicated by the symbol "*" in this description (Fu et al., 2020; Sukanya et al., 2022).

Volmer–Heyrovsky (V–H) Mechanism: In contrast to the V-T process, after the Volmer step, the Heyrovsky step occurs when H^+ in the electrolyte and another transmitted electron from an external circuit combine with the H^*_{ads}, thereby forming H_2 gas as shown in table 1(in acidic solution). In basic media, after the volmer step, the water molecule (H_2O) and the transmitted electron are combine with the $H^*_{ads}$to form the H_2 and OH^- in the Heyrovsky step (table 1) (Fu et al., 2020; Sukanya et al., 2022).

Table 1: Her Mechanisms in both Acidic and Basic Media

Mechanisms	Acidic Medium	Basic Medium
Volmer Step	$* + H^+ + e^- \rightarrow H^*_{ads}$	$* + H_2O + e^- \rightarrow H^*_{ads} + OH^-$
Tafel Step	$2H^*_{ads} \rightarrow H_2 + 2^*$	$2H^*_{ads} \rightarrow H_2 + 2^*$
Heyrovsky Step	$* + H^+ + e^- + H^*_{ads} \rightarrow H_2 + *$	$* + H_2O + e^- + H^*_{ads} \rightarrow H_2 + OH^- + *$

Furthermore, it can be seen that HER is a pH-dependent response as well (table 1). There are some changes between the processes in basic and acidic solutions, particularly in the Volmer and Heyrovsky Steps as shown in table 1. Since there is an abundance of H^+ in acidic solutions, the hydrogen adsorption sites can readily acquire protons by the Volmer reaction. The HER process is hampered when the alkaline medium is utilized as the electrolyte since there are no enough protons available. As a result, water molecules (H_2O) must serve as the proton donor for the succeeding reactions, which will first split into H^+ and OH^-. This is the reason why HER reacts slowly in basic media (Wei et al., 2018;Yu et al.,2013). Normally, high overpotentials are needed in basic/alkaline solutions due to the sluggish kinetics of the HER and this remains a challenge in the development of active and stables HER electrocatalysts in alkaline media (Faid et al., 2021).

Oxygen Evolution Reaction (OER)

OER is one of the two half reactions that take place during the electrocatalytic splitting of water process. It occurs at the anode and is given by equation 1(acidic media) and equation 2 (basic media).

$$2H_2O \rightarrow 4H^+ + 4e^- + O_2 \quad (1)$$

$$4OH^- \rightarrow 2H_2O + O_2 \quad (2)$$

However, OER involves the transfer of four protons coupled with four electrons and bond breakage and

formation, as such much higher applied potentials are needed for the production of O_2, leading in high overpotentials (Sukanya, et al., 2022). It is the more kinetically demanding counter-reaction to the HER when splitting H_2O into hydrogen and oxygen using electricity. Frankly, the entire efficiency of the electrocatalytic water splitting reaction in an electrochemical cell is usually limited by the OER. Moreover, the mechanism of OER is complex and strongly relies on the nature of the electrocatalyst, the most commonly used mechanism for the OER is called the Adsorbate Evolution Mechanism (AEM). In AEM, the first step (in alkaline solution) is the adsorption of OH^- at an adsorption site (*), to produce the adsorbed OH^*_{ads} (equation 3). The OH^*_{ads} intermediates then further combine with OH^- to form H_2O and adsorbed O^*_{ads} atoms, (equation 4). This is followed by the formation of adsorbed OOH^*_{ads} (equation 5), which then reacts with additional OH^- to give O_2 and H_2O (equation 6).

$$* + OH^- \rightarrow OH^*_{ads} + e^- \quad (3)$$

$$OH^*_{ads} + OH^- \rightarrow O^*_{ads} + H_2O + e^- \quad (4)$$

$$O^*_{ads} + OH^- \rightarrow OOH^*_{ads} + e^- \quad (5)$$

$$OOH^*_{ads} + OH^- \rightarrow * + O_2 + H_2O + e^- \quad (6)$$

Parameters to be Considered When Choosing a Good Electrocatalyst

The descriptors of a good electrocatalyst material are discussed briefly as follows:

Surface area

This is one of the best indicators in assessing the electrocatalytic activity of a material. Materials with high values of surface area exhibit more electrocatalytic activity. This is because; the value translates to the approximate information about the quantity of active sites on the surface of the catalysts. Even though possibly not all sites could show catalytic activity, the surface area can still serves as a reference for evaluating the performance of electrocatalysts in the HER and OER processes (Lin et al., 2019;Dang et al., 2018;Zhang et al., 2015). However, TMDs are characterized by having a large surface area with the bulks TMDs having lower surface area in comparison to their nano-sized/thin counterparts.

Gibbs Free Energy Change (ΔG_{H^*} and ΔG_{OH}^* for acidic and alkaline media respectively)

It is obvious that hydrogen adsorption is intermediary step in both V-T and V-H mechanisms of the HER process, as such Gibbs free energy of hydrogen atom adsorption (**ΔG_{H^*}**) is considered as only essential descriptor to screen the performance of the acidic HER electrocatalyst (Liu et al., 2019). That is why many previous computational studies have only focused on it (Lin et al., 2020; Prabhu, 2020;Wu and Hofmann, 2021). However, recent works have stressed the need of including the hydroxyl (OH) adsorption Gibbs free energy changes (ΔG_{OH}^*) as another important indicator for the alkaline HER catalysts' design (McCrum and Koper, 2020;Ogunkunle et al., 2024). Based on the Sabatier plot (which is also called the Volcano plot) shown in figure 4, the free energy for adsorption of reactants and reaction intermediates should be neither too low nor too high ($\Delta G_{H^*} \approx 0$, i.e., is the idealist value) (Chen et al., 2017; Koper, 2013; Nørskov et al., 2005).

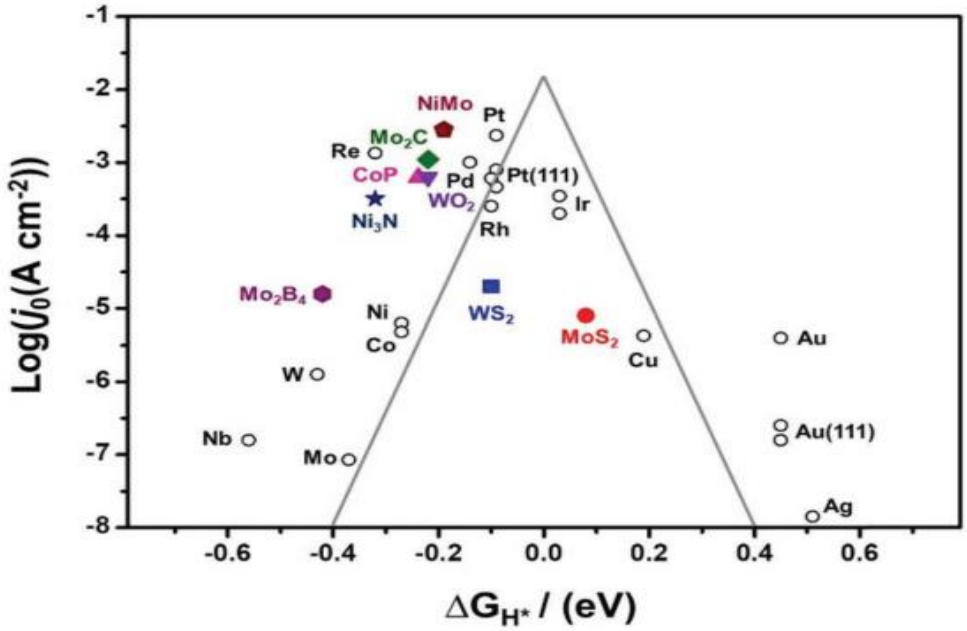

Figure 4: Sabatier plot that shows the relationship of exchange current density of some materials and their corresponding ΔG_{H^*} obtained from reference (Yu et al., 2019)

It was reported that the Pt-groups have their hydrogen (H) and hydroxyl (OH) adsorption Gibbs free energy (ΔG_{H*} and ΔG_{OH}^{*}) values around 0.0 eV and – 0.3 eV respectively (Yu et al., 2019;McCrum and Koper, 2020). Thus, for a material to be good in HER process, its ΔG_{H*} and ΔG_{OH}^{*} should be very close to these values. This is why, MoS_2, as typical TMDs, with a modest value of ΔG_{H*} (which is close to the Pt-groups) is considered as a highly efficient HER electrocatalyst (figure 7). Theoretically, ΔG_{H*} and ΔG_{OH}^{*} can be computed using the following relations (Huang et al., 2022; Ogunkunle et al., 2024).

$$\Delta G_{H^*} = \Delta E_{H^*} + T\Delta S + \Delta ZPE \quad (8)$$

Where ΔE_{H^*} is the adsorption energy of H atoms, which can be calculated from the following equation:

$$\Delta E_{H^*} = E_{H^*} - E_* - \frac{1}{2}E_{H_2} \quad (9)$$

Where, E_{H^*} and E_* are the energies of the TMD monolayers with and without absorbed H atoms, respectively and E_{H_2} is the energy of the free H_2 molecule. T, ΔS, and ΔZPE in equation (8) are the room temperature (T = 298.15 K), entropy change, and zero-point energy change, respectively, whose values can be obtained from the literatures (Huang et al., 2022;Dong et al., 2018;Skulason et al., 2010;Huang and Li, 2019).

However, the ΔG_{OH}^{*} can be computed as follows:

$$\Delta G_{OH^*} = \Delta E_{OH^*} + T\Delta S + \Delta ZPE \quad (10)$$

Where, ΔE_{OH^*} is the adsorption energy of OH and can be calculated as follows:

$$\Delta E_{OH^*} = E_{OH^*} - E_* + E_{H_2O} + \frac{1}{2}E_{H_2} - 2E_{H_2O} \quad (11)$$

E_{OH^*} is the energies of the monolayer with adsorbed OH, and E_{H_2O} is the energy of an isolated water molecule.

Overpotential (η)

Overpotential is another descriptor for assessing the performance of electrocatalysts in the HER process. In practical situation, the value of ΔG_{H*} is either greater or lower than zero which implies that a thermodynamic overpotential is required to drive the HER process (Fu et al., 2020). The excess voltage needed to drive the HER above its thermodynamic potential is referred to as the overpotential. In other words, it's the extra energy required to get past the kinetic barriers and speed up the reaction. However, since the overpotential in HER directly influences the amount of energy needed for the reaction, reducing it is essential to increasing the sustainability and efficiency of hydrogen production. As such, researchers concentrate on creating sophisticated electrocatalysts and refining reaction conditions to reduce overpotential and improve HER performance as a whole. Therefore, an excellent electrocatalyst should produce hydrogen gas at a lower overpotential value.

Exchange Current Density (i_0)

Exchange current density (i_0) is another outstanding parameter that describes the electrocatalytic activity of a material. The current density at which there is no net current flow and the rates of the forward and reverse reactions are equal is known as the exchange current density. The exchange current density in HER, denoted by $\boldsymbol{i_0}$, is the point at which hydrogen evolution and oxidation events happen simultaneously. However, improved electrocatalytic activity and quicker reaction kinetics are indicated by a larger exchange current density. The units used to measure $\boldsymbol{i_0}$ are usually mA/cm² or A/cm². One of the challenges now is to create electrocatalysts that can enhance the efficiency and performance of hydrogen evolution reactions by having a high exchange current density.

Theoretically, $\boldsymbol{i_0}$ can represent the rate of the proton transfer to the surface, which can be derived on the basis of ΔG_{H^*}. At standard conditions (pH = 0 and T = 300 K), the i_0 can be computed using equations (12) and (13) when the proton transfer is exothermic ($\Delta G_{H^*} < 0$) and endothermic ($\Delta G_{H^*} > 0$) respectively (Nørskov et al., 2005).

$$i_0 = \frac{-ek_0}{1+exp\left(\frac{-\Delta G_{H_*}}{KT}\right)} \quad (12)$$

$$i_0 = \frac{-ek_0 exp\left(\frac{-\Delta G_{H_*}}{KT}\right)}{1+exp\left(\frac{-\Delta G_{H_*}}{KT}\right)} \quad (13)$$

Where k_0 is the rate constant (200 s^{-1}/site) and K is the Boltzmann constant.

Tafel Slope

The Tafel slope (b) is a crucial metric in electrocatalysis that characterizes the relationship between the logarithm of the catalytic current density ($\log i$) and the overpotential (η) for an electrochemical process. The Tafel slope can be described by the Tafel equation which is given as (Gileadi and Kirowa-Eisner, 2005).

$$\eta = \pm b \log\left(\frac{i}{i_0}\right) \quad (14)$$

Where, η is the overpotential, i_0 is the exchange current density, b is the Tafel slope and i is the catalytic current density. The +/- sign seen in the equation relates to whether the analysis refers to an anodic (+) or cathodic (-) process.

The Tafel slope b (mV dec^{-1}) could be written as:

$$b = \frac{2.3RT}{\alpha nF} \quad (15)$$

Where, R and F represent ideal gas constant (8.314 J mol^{-1} C^{-1}) and Faraday constant (96 485 C mol^{-1}), respectively. T, α, and n represent Kelvin temperature, electrochemical transfer coefficient, and electrons that transferred, respectively.

However, Tafel slope is typically used to determine the rate-determining step (RDS) for the V-T and V-H mechanisms as discussed above (Chen, et al., 2017;Wu

et al., 2019). The Tafel slope at room temperature for the Tafel, Heyrovsky and Volmer steps were determined to be around 30, 40, and 120 mV dec^{-1} respectively (Tian et al., 2019). According to the computed Tafel slope, the Volmer reaction is the RDS and the hydrogen atoms are too slow to be adsorbed on the catalyst surface if the b is more than 120 mV dec^{-1}. The Heyrovsky reaction becomes the RDS and the hydrogen atom can be adsorbed more quickly on the catalyst surface but will desorb slowly if the b is between 40 and 120 mV dec^{-1}. Nonetheless, the Tafel reaction will be recognized as the RDS if the value of b comes out to be roughly 30 mV dec^{-1} (Fu et al., 2020). A smaller Tafel slope denotes a more effective electrocatalyst since it signifies faster kinetics.

TMDs – Based Electrocatalyst

Jaramillo and his co-researchers used Scanning Tunneling Microscopy (STM) experiments to demonstrate the catalytic activity of TMDs edge sites (Jaramillo, et al., 2007). The basal plane of TMDs – which is the majority of their surface area, is considered to be catalytically nonreactive (Kuc et al., 2015). Researchers have developed various methods of overcoming this issue of non-reactivity of the basal plane (Tsai et al., 2017;Ouyang et al., 2016;Gao et al., 2016). However, the edge planes or defective basal planes are usually preferred for catalytic applications due to their higher reactivity. Thus, several works were reported on the activation of edge sites in TMDs (Kibsgaard et al., 2012).

Table 2 below shows comparison between electrocatalytic activities of different TMDs-based electrocatalysts. It is important to note that among the TMDs-based electrocatalysts that were reported, MoS_2 is the most studied electrocatalyst (Jaramillo et al., 2007; Lukowski et al., 2013; Li et al., 2011;Tsai et al., 2017;Ouyang et al., 2016 ;Gao et al., 2016). Even though these materials exhibit some electrocatalytic properties comparable to those of the precious Pt-groups, still their catalytic activities need to be improved for effective HER process.

Table 2: Comparison of the Electrocatalytic Ability of Some Available TMDs-Based Electrocatalysts.

TMDs-Based Electrocatalyst	Solution	$\Delta G_{H^*}/\Delta G_{OH^*}$ (eV)	η (mV)	Current Density ($mAcm^{-2}$)	i_0 ($mA\ cm^{-2}$)	Tafel slope ($mV\ dec^{-1}$)	References
1T MoS_2	acidic	-	100	10	-	40	Voiry et al., 2013
1T MoS_2	acidic	-	187	10	-	43	Lukowski et al., 2013
N-MoS_2	acidic		168	10	-	40.5	Li et al., 2017
1T' MoS_2	acidic/alkaline	0.29/1.78	-	-	-	-	Ogunkunle et al., 2024
1T' $MoSe_2$	acidic/alkaline	1.81/1.65	-	-	-	-	Ogunkunle et al., 2024
1T' WS_2	acidic/alkaline	0.43/1.85	-	-	-	-	Ogunkunle et al., 2024
1T' WSe_2	acidic/alkaline	0.92/1.76	-	-	-	-	Ogunkunle et al., 2024
Fe-MoS_2	acidic/alkaline	-	88/92	-	-	75/49	Vikraman et al., 2022
1T/2H $MoSe_2$	acidic	-	192	10	-	48	Shi et al., 2021
MoS_2	acidic	-	300	10	126.5	55	Xie et al., 2013
V-WS_2	acidic	-	148	10	0.33	71	Jiang et al., 2018
ReS_2	acidic	-	142	10	-	64	Li et al., 2016
VS_2	acidic	-		10	-	159	Chia et al., 2016
CoS_2	acidic	-	197	10	-	29.9	Jaberi et al., 2021
TaS_2	acidic	-	200	10	-	135	Li et al., 2016
FeS_2	acidic	-	217	10	1.44×10^{-4}	56.4	Faber et al., 2014
Mn-$CoSe_2$	acidic	-	174	10	6.83×10^{-2}	36	Liu et al., 2016

Some Strategies of Improving the Catalytic Activity of TMDs-Based Electrocatalysts

The catalytic activities of TMDs can also be enhanced through: Doping, formation of Janus TMDs, construction of heterostructures among others.

Doping

Doping as one of the strategies of improving the electrocatalytic activities of TMDs, creates more active sites for catalysis, increases the conductivity and decreases the value of Gibbs free energy of hydrogen adsorption (ΔG_{H*}) leading to higher hydrogen evolution reaction (HER) performance. Several works were reported in relation to the doping of TMDs for enhanced HER performance using both metal and nonmetal dopants. It was reported that Vanadium atom doping on the MoS_2 nanosheets enhances its conductivity but decreases the density of active sites (Sun et al., 2014). However, it was common practice to dope MoS_2 with Ni and Co to increase its HER activity (Zhang et al., 2014;Bonde et al., 2009;Lv et al., 2013). These two dopants have the potential to lower ΔG_{H*} and raise the density of active sites, hence improving HER performance. Co-doped MoS_2 was prepared by Xiong et al. via a one-step hydrothermal process (Xiong et al., 2018), and when compared to pure MoS_2, it showed increased HER catalytic activity. In alkaline media, the sample Co-MoS_2-0.5 showed the greatest HER performance when the doping amount of Co source was 0.5 mmol. The decrease in ΔG_{H*} and the controlled electronic structure brought about by Co doping are responsible for this improvement.

Additionally, a wide variety of nonmetal-doped TMDs exhibit distinctive characteristics and superior HER performance. In contrast to the metal doping approach, nonmetal doping produces crystal distortion or an amorphous structure with lots of active sites in addition to optimizing the ΔG_{H*}(Wang et al., 2019;Fu et al., 2015;Yang et al., 2015). A study based on DFT revealed that high Phosphorus (P)-doping concentrations on the tungsten-based dichalcogenides (WS_2 ,WSe_2 and WTe_2) can enhance the number of active sites and exhibit a suitable ΔG_{H*} (Huang, et al., 2022).

By using a hydrothermal process, Xie et al. created MoS_2 nanosheets doped with oxygen(Xie et al., 2013). A tiny amount of Mo–O bonds were inherited by MoS_2 nanosheets as a result of the relatively low synthesis temperature. Additionally, the DFT results showed that the bandgap of MoS_2 slab combined with oxygen was 1.30 eV shorter than the value of 2H MoS_2 slab, which is 1.75 eV. The oxygen insertion into MoS_2 nanosheets produced this bandgap narrowing effect by increasing the carrier concentration and improving conductivity. The outcome was an optimized oxygen-incorporated MoS_2 catalyst with a Tafel slop of 55 mV dec^{-1} and a overpotential (η) of 120 mV (at 1 mA cm^{-2}).

Furthermore, Jin's group discovered that doping with chlorine (Cl) improved the HER activity of both MoS_2 and $MoSe_2$ catalysts and adjusted the electronic structure of the amorphous $MoSe_2$ and MoS_2 (Ding et al.,2015;Zhang et al., 2015). Ultimately, the multiple active sites and ideal electronic structure improved MoS_xCl_y and $MoSe_xCl_y$'s HER performance (Ding et al., 2015). However, the dopants still need to be carefully chosen because different atoms would have different effects on catalytic activity and improper elements could even have a negative effect on the final performance (Fu et al., 2020). Another confusing result is that the HER catalytic activities can show different results, sometimes even inversed, even after doping with the same elements (Shi et al., 2017;Zhang et al., 2014). This may be due to different preparation methods and doping amounts cause the dopants to anchor on different sites of the TMDs. However, more theoretical and experimental research is needed to understand the underlying mechanism (Fu et al., 2020).

Formation of Janus TMDs

In the recent years, much interest and focus have been made on asymmetric TMDs, which are known as Janus TMDs, with an asymmetric X–M–Y structure, such as TeMoSe, as shown in the schematic in figure 5. In Janus TMDs, the transition metal layer (M) is sandwiched between two different chalcogen layers (X and Y) and this leads to a decrease in structural symmetry, which in turn can give rise to different electronic and optical properties (Sukanya et al., 2022). These Janus TMD layers are also attracting considerable attention in both electrocatalysis (He et al., 2021; Kaur and Kumar, 2021) and photocatalysis (Idrees et al., 2020). Because they exhibit an improved catalytic activity compared to the non-janus TMD materials. However, the asymmetric structure gives rise to an intrinsic dipole moment due to the different electronegativities of the two chalcogen atoms. The layer with the lower electronegativity will become positively charged, whereas the layer with the higher electronegativity will be negatively charged (Sukanya, et al., 2022). Dipole moments and electrostatic potentials for a range of Janus TMDs were computed by Ji and his co-researchers (Ji et al., 2018). The dipole moments of 0.19 D and 0.77 D were reported for SMoSe and OMoTe respectively, with the higher dipole due to the greater difference in electronegativity of the O and Te atoms. Also, surface potential differences as high as 0.77 eV and 3.26 eV were computed for SMoSe and OMoTe respectively, and these are sufficient to cause electronic band bending.

However, according to research, the structural asymmetry in Janus TMDs causes electrons to redistribute, which increases charge accumulation on metal atoms and raises catalytic efficiency (Wang et al., 2022; Er et al., 2018). An encouraging substitute for

precious metal catalysts, research has demonstrated that anchoring transition metals on Janus MoSSe surfaces can result in efficient single-atom catalysts for HER and OER applications (Wang et al., 2022; Paez-Ornelas et al., 2021). Furthermore, without necessitating appreciable strain or vacancy concentrations, the introduction of in-gap states and changes in the Fermi level brought about by Janus asymmetry boost intrinsic catalytic performance (Er et al., 2018). These results imply that Janus TMDs are not only feasible but also possibly better options for a range of catalytic uses in energy storage and conversion technologies. It should be highlighted, nonetheless, that the Janus TMDs with two distinct chalcogen surfaces are much harder to make experimentally and are usually made via modified chemical vapour deposition (CVD) methods (Zhang et al., 2020).

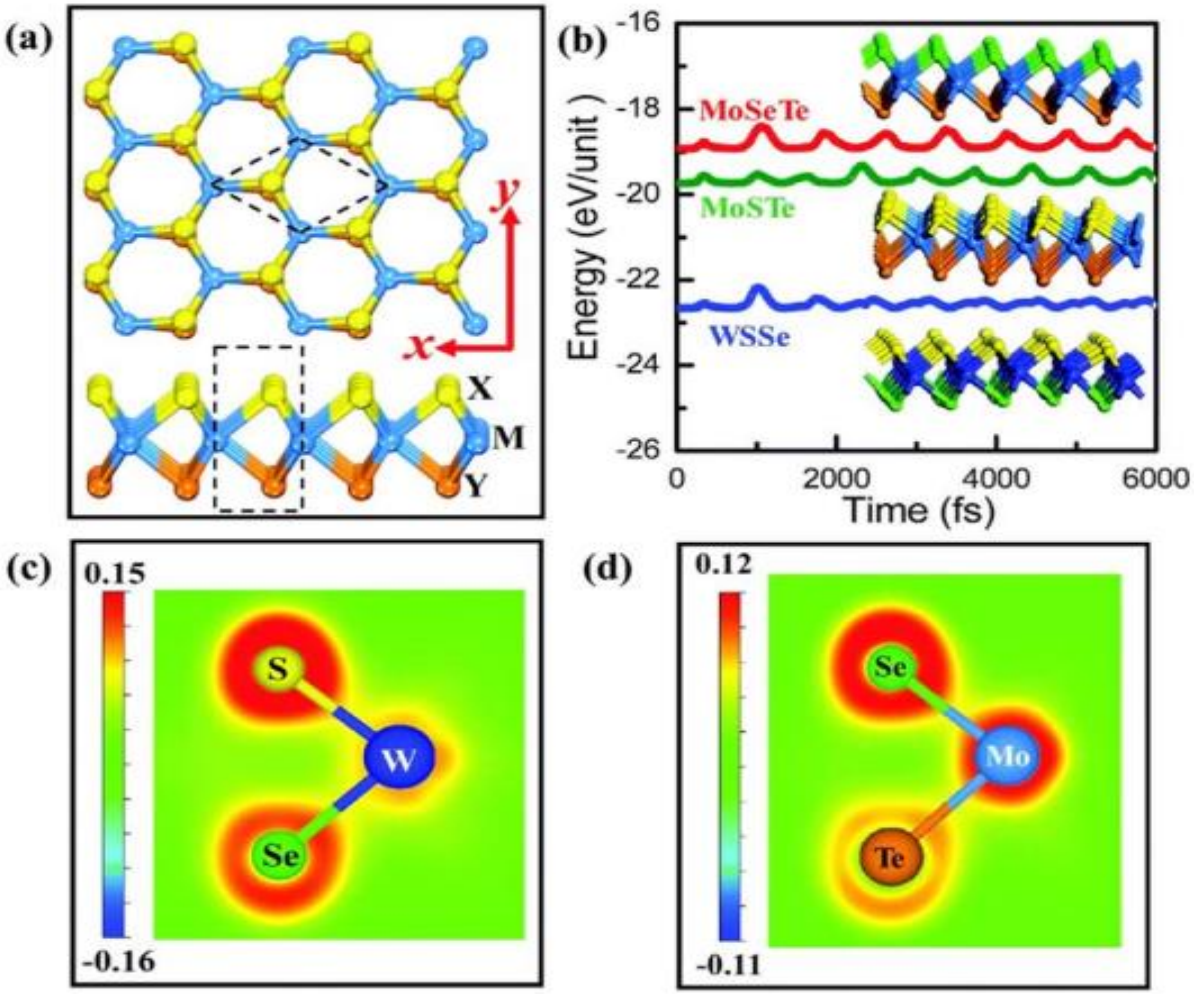

Figure 5: Representation of Janus TMDs: (a) Layered Structure of Janus TMDs (b) Plot of energy versus time of some Janus TMDs (c) Charge density plot of Janus WSSe (d) Charge density plot of Janus MoSeTe, obtained from reference (Wang et al., 2018)

Construction of Heterostructures

TMD heterostructures are also considered as new materials with interesting properties. In these materials, different TMD monolayers are coupled by weak van der Waals forces to form heterostructures, such as $MoSe_2/WS_2$ (Vikraman et al., 2021). Heterostructures have a band alignment whereby the conduction band minimum (CBM) and valence band maximum (VBM) are situated in different monolayers. This leads to the formation of interlayer excitons and boosts interlayer charge transfer, thereby providing a new avenue to engineer more efficient electrocatalysts (Sukanya et al., 2022).

Moreover, preparation of heterostructures made up of TMDs and their corresponding transition metals oxides has also gained more attention. Chen et al. created MoO_3/MoS_2 nanowires, in which the two materials are arranged in a core/shell configuration (Chen et al., 2011). They discovered that this design produced an architecture with notable stability during HER catalysis as shown in figure 6a, with the core acting as a conducting scaffold for the MoS_2 catalyst shell (Chen et al., 2011). The MoS_2

nanoparticles on a reduced graphene oxide (RGO) substrate were synthesized by Li and his co-researchers (Li et al., 2011). When compared to either MoS_2 nanoparticles or the RGO alone, the electronic and chemical interaction of the RGO and MoS_2 was observed to generate improved electrocatalytic activity toward the HER as seen in figure 6b. The study's solvothermal synthesis technique preserved the TMD's catalytic activity while preserving the one-dimensional structures' porosity and conductivity. In comparison to nanorods made entirely of MoO_2 or WO_2, porous nanorods with MS_2/MO_2 (M= W or Mo) heterointerfaces exhibit a lower overpotential and a higher current density when used as HER catalysts as depicted in figure 6c (Wang et al., 2016).

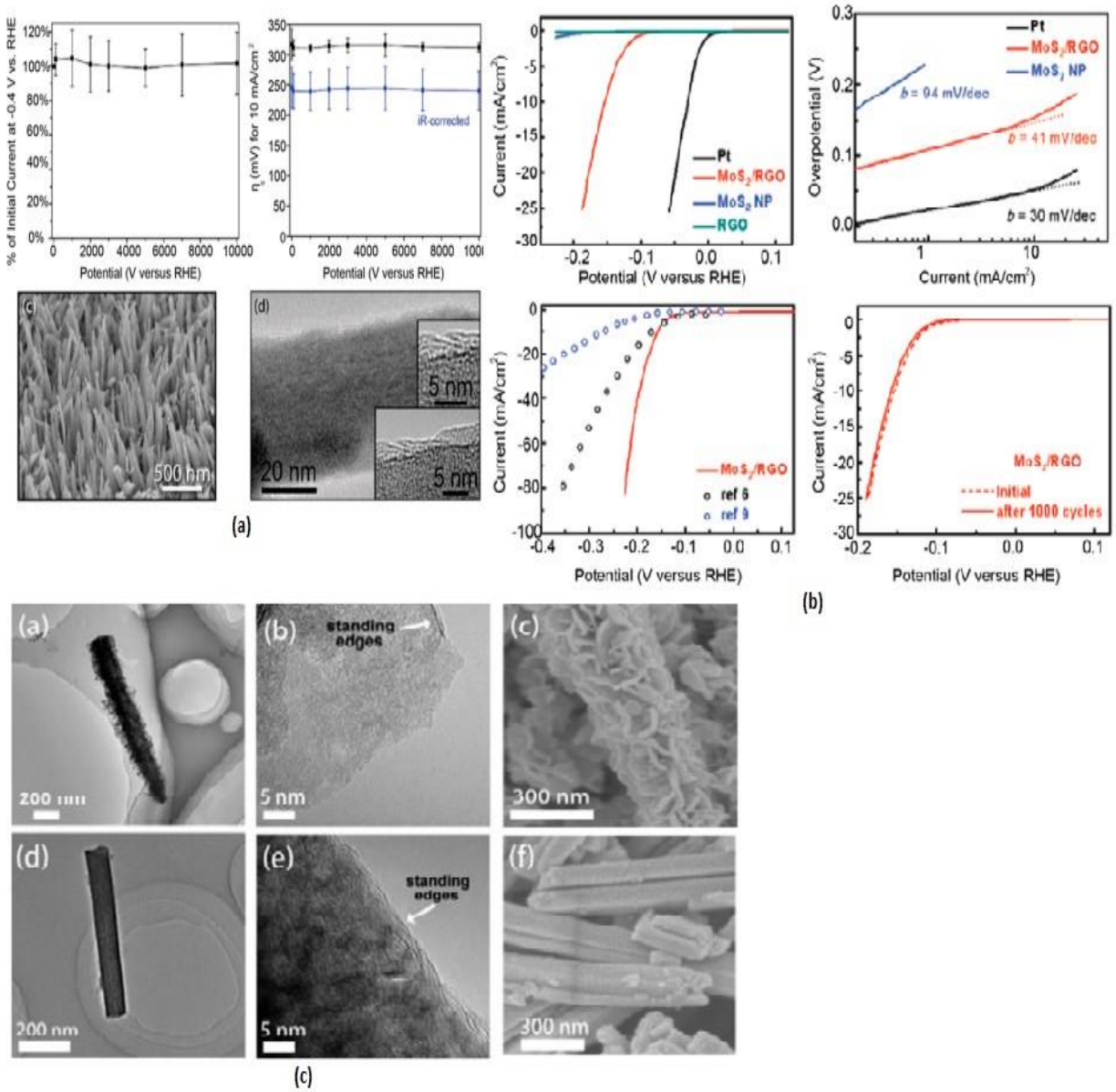

Figure 6: Catalytic Properties of TMDs (a) Plots showing the excellent stability of MoO_3/MoS_2 nanowires during HER catalysis over 10,000 cycles and electron microscopy images of MoO_3 (core)−MoS_2 (shell) nanowires reproduced from reference (Chen et al., 2011) (b) Plots of current−voltage attesting to the lower overpotential and smaller Tafel slope of MoS_2 crystals when supported on reduced graphene oxide (RGO) reproduced from reference (Li et al., 2011) (c) Micrographs of layered WS_2 decorating WO_2 nanorods (top) and layered MoS_2 decorating MoO_2 nanorods reproduced from reference (Wang et al., 2016).

Methods Used To Synthesize Tmds-Based Electrocatalysts

Since the layered structure of TMDs-based electrocatalysts is largely responsible for their excellent catalytic performance, the synthesis of layer-controllable TMDs materials with large-area uniformity is essential to their wide range of practical applications (Fu et al., 2020). Generally, there are two main approaches used for preparing TMDs-based electrocatalysts, namely:

i. Top - Down Approach
ii. II. Bottom - Up Approach

Top - Down Approach

Top-down approach involves breaking down bulk TMD materials into nanoscale structures or single layers. This method uses TMDs that have already been synthesized as precursors, and then transfers them to the necessary substrates using various techniques. Therefore, in top-down methods, TMDs materials are not synthesized from constituent elements but only transferred from one substrate to another (Mehta et al., 2024). One of the widely known techniques is called mechanical exfoliation. This technique physically separates layers from bulk TMDs, yielding high-quality materials but often at low yield rate to satisfy the application in practical electrocatalysis (Li and Xue., 2016; Cao et al., 2019). Thus, it is more appropriate for some mechanism investigations or the fabrication of devices (Fu et al., 2020).

However, for scalable production of layered TMDs-based electrocatalysts, lithium insertion is proposed. This process of lithium insertion does not only reduce the number of layers of the bulk TMDs, but also creates some structural changes in TMDs which subsequently lead to improved catalytic activity. There are three methods of lithium intercalation that are commonly used. Firstly, there is chemical exfoliation method using organolithium compounds such as butyllithium (BuLi), methyllithium (MeLi), or lithium borohydride ($LiBH_4$) (Ambrosi et al., 2015;Voiry et al., 2013) as depicted in figure 7a–c. Only that this method consumes a lot of time, and the final result was sometimes unsatisfying. The second method that was proposed is called electrochemical lithium insertion method. This method exhibits some advantages over the first one, including the fact that the lithium insertion was carried out in a lithium battery test cell as shown in figure 7d. Nevertheless, this method still has some drawbacks, including a complex process that requires the assembly of battery cells and the possibility of impurities being introduced into the final products due to additional additives that are typically used during the electrode fabrication process (Tan et al., 2017).

Recently, a novel process called liquid ammonia-assisted lithiation (LAAL) technique for the exfoliation of bulk TMDs was introduced (Fu et al. (2020). This method proved to be an effective means of obtaining ultrathin 2D nanosheets (Yin et al., 2016;Yin et al., 2014). Lithium metal must first be placed within a quartz tube that is protected from air by argon (Ar) in order to perform the LAAL procedure as shown in figure 7e. After that, the tube is removed and submerged in a bath of liquid nitrogen. A very pure ammonia gas is added at the same time, and it eventually condenses into a liquid state. The lithiation reaction starts as soon as the powder is submerged in liquid ammonia, and the color of the liquid progressively changes from blue to colorless, serving as a gauge for the reaction progress. Through meticulous evaporation, ammonia gas is extracted from the tube once the "blue color" has fully disappeared. The ultrathin 2D nanosheets are also generated by adding water into the sample that has been intercalated with lithium as seen in figure 7f–h.

Conclusively, though top-down approaches were proved to be among the methods of obtaining layered-TMDs from the bulk materials and despite all the efforts being made to improve them, they still suffer from different challenges which limit their applicability in producing TMDs-based electrocatalysts with appreciable properties such as regular morphologies and controllable layer number. As such, they are popularly use in the fabrication of devices (Mehta et al., 2024).

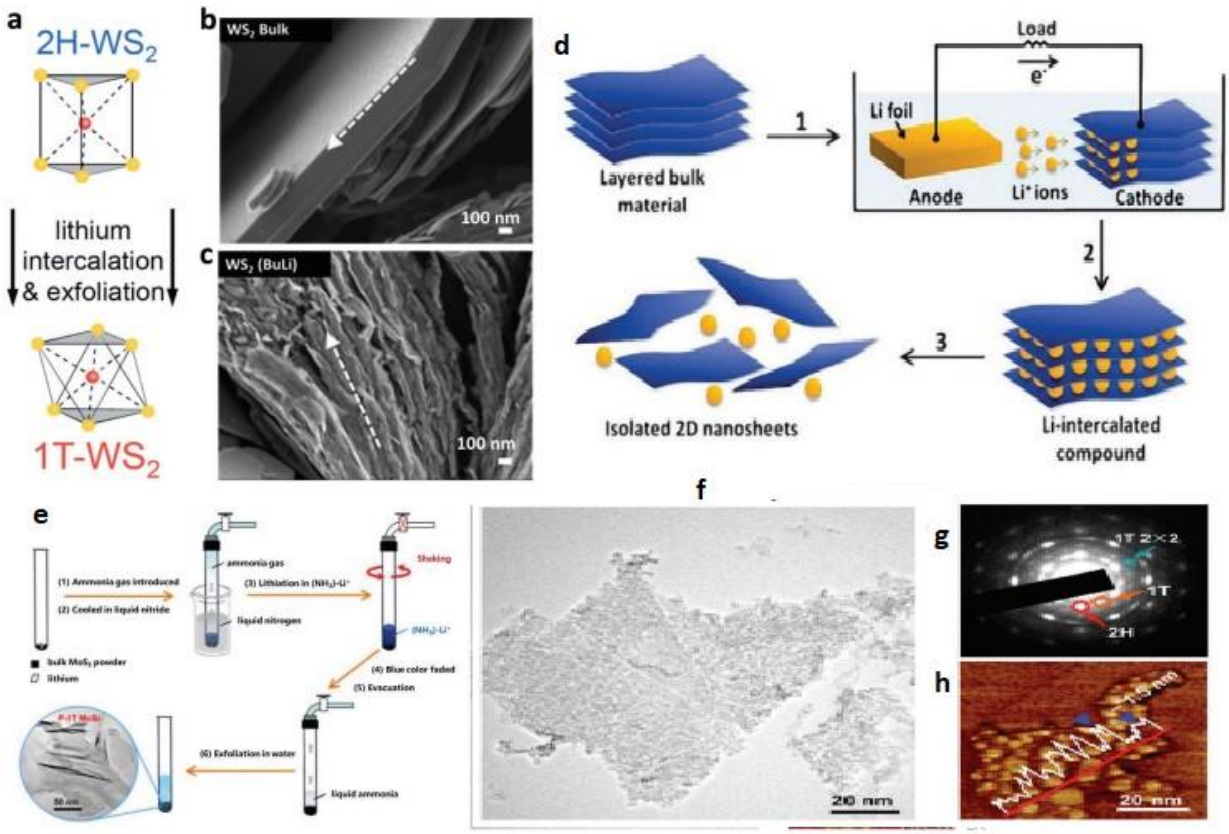

Figure 7: Three commonly used lithium-insertion methods to obtain layered TMDs materials NSs. (a) Exfoliating the bulk WS_2 with organolithium compounds to produce 1T WS_2 NSs. Reproduced (Lukowski et al., 2014) (b) The SEM images for the bulk WS_2 and (c) after the BuLi treatment with subsequent exfoliation in water Reproduced (Eng, et al., 2014) (d) Fabrication of 2D NSs from the layered bulk material with electrochemical lithiation process Reproduced feom (Zeng et al., 2011) (e) A diagrammatic drawing of LAAL processes.(f) Morphology of mesoporous 1T MoS_2 NSs. (g) The corresponding SAED pattern and (h) atomic force microscopy (AFM) image of exfoliated MoS_2 NSs. (e–h) Reproduced from (Yin et al., 2016)

Bottom - Up Approach

Bottom-up methods deal with the synthesis of materials from molecular or atomic precursors. The common techniques are:

Chemical Vapor Deposition (CVD)

This is a widely used method that allows for the growth of TMDs on substrates through chemical reactions in vapor phase (Mehta et al., 2024; Yu et al., 2024). Halogen-containing gases, such as hydrogen sulfide (H_2S), or a gaseous chalcogen made by evaporating chalcogen powder are used as chalcogen precursors in this method. However, the CVD of TMDs can be achieved by the vapor-phase reaction of evaporated metal oxides with gaseous chalcogens or by the direct chalcogenization of pre-deposited thin films of metal (or metal oxide) as shown in Fig. 8(a), (Shim et al., 2017). Thin TMDs are synthesized in a chalcogen environment at high temperatures (>700$^{\circ C}$). TMDs materials produced by this method are characterized by having high surface area, homogeneous thickness, high crystallinity, and superior electrochemical performance (Tanwar et al., 2021). The method also makes it possible to modify and adjust the value of ΔG_H, create a large number of edge sites all of which contribute towards enhancing the HER catalytic performance (Shim et al., 2017; Chen et al., 2016;Zhang et al., 2017). However, modified CVD techniques are usually used to produce the Janus TMDs, which are much more difficult to form experimentally (Zhang et al., 2020).

Hydrothermal Method

The hydrothermal method is the most popular bottom-up technique for creating nanomaterials due to its cost-effectiveness, ease of use, quick synthesis, high yields, high purity, low environmental impact and versatility in creating various hybrid materials (Baig et al., 2021;Dhand et al., 2015). It is often carried out at high temperatures and pressures in closed vessels, as illustrated in Fig. 8(b). TMDs synthesized at higher

temperatures and pressures exhibit improved crystallinity, phase purity, and distinctive morphologies (Swain et al., 2021;Tanwar et al.,2021). In hydrothermal method, water and organic/inorganic solvents are utilized as reaction medium to dissolve precursor materials. The common precursors employ in this method include inorganic salts and metal oxides, particularly; molybdenum and selenium sources such as Na_2MoO_4 and $Na_2S_2O_3$. TMDs in a range of shapes, including nanoflowers, nanoflakes, nanoplates, nanoparticles, and quantum dots, can be created by hydrothermal synthesis Sukanya et al., 2022). For instance, Ni-doped $MoSe_2$ nanoplates were created by dissolving Na_2MoO_4 and $Ni(NO_3)_2$ in water, then adding selenium and hydrazine drop by drop over the course of 30 minutes. In an autoclave, the reaction mixture was then kept at 180 °C for 12 hours (Sakthival et al., 2019). It was also discovered that $MoSe_2$ nanosheets made by hydrothermal reaction were an effective HER catalyst. The products would exhibit varying crystal phases and degrees of disorder if the reaction temperature, as well as the ratio of $NaMoO_4{\cdot}2H_2O$ and Se precursors to the reductant ($NaBH_4$), were adjusted (Yin et al., 2017). To create a variety of ternary composite materials for a range of uses, researchers have also employed hydrothermal synthesis processes (Shen et al., 2016;Shifa et al., 2016;Naz et al., 2019).

However, despite the fact that hydrothermal reaction is a prominent method for creating nanostructured materials, but it has some drawbacks and one of them is that the products might be readily oxidized during the process, either from the solution or from the environment, which could affect the purity of the materials. As such, when creating TMD-based nanomaterials, the solvothermal reaction is used to prevent potential oxidation (Gao et al., 2015;Xu et al., 2015).

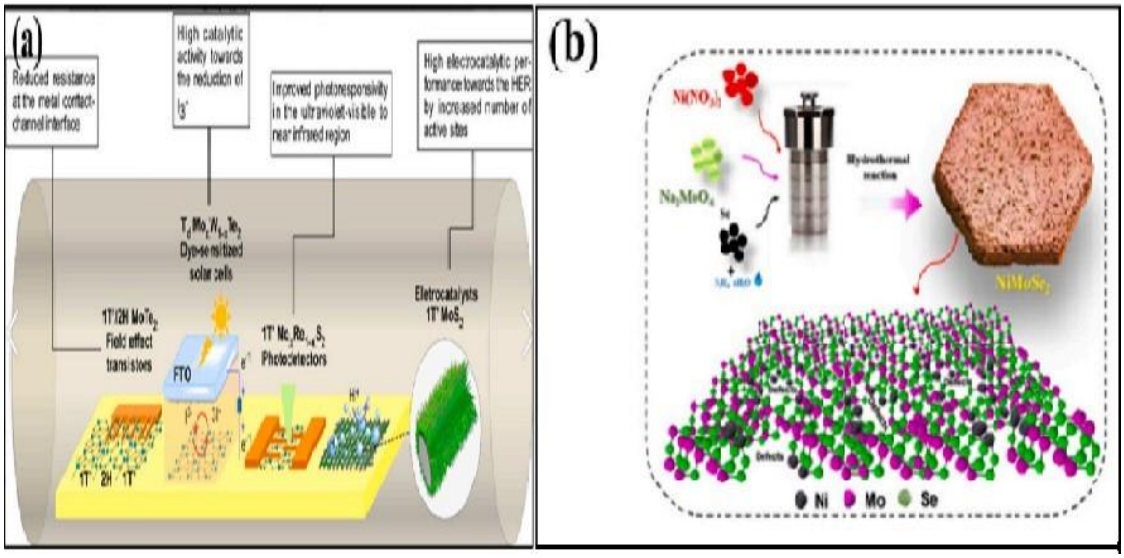

Figure 8: Schematic Illustration of Different Methods Based on Bottom-up Approach (a) chemical vapor deposition, adapted from Ref.(Hermandez Ruiz et al., 2022) (b) hydrothermal method from Ref. (Sakthival et al., 2019).

Solvothermal Method

This method involves chemical reactions in a solvent under high temperature and pressure, enabling the formation of TMD nanostructures (Mehta et al., 2024; Yu et al., 2024). Solvothermal technique is similar to the hydrothermal approach; the main difference is that the solvent in the hydrothermal method is aqueous, whereas the precursor solution in the solvothermal method is not. Depending on the kind of material being created, solvothermal synthesis can produce desirable characteristics and better morphology than hydrothermal synthesis. The advantages of hydrothermal synthesis and sol–gel are combined in the Solvothermal approach (Swain et al., 2021; Tanwar et al., 2021). Various precursors are used for the solvothermal synthesis, such as sodium molybdate dihydrate ($Na_2MoO_4{\cdot}2H_2O$), citric acid monohydrate ($C_6H_8O_7{\cdot}H_2O$), copper (II) acetate monohydrate ($Cu(CH_3\ COO)_2{\cdot}H_2O$), thiourea ($CH_4N_2S$), stannic chloride pentahydrate ($SnCl_4.5H_2O$), graphite powder, sodium nitrate ($NaNO_3$), potassium permanganate ($KMNO_4$), ammonium heptamolybdate ($(NH_4)_6Mo_7O_{24}$), silicon dioxide (SiO_2), tungsten chloride (WCl_6), cadmium nitrate tetrahydrate ($Cd(NO_3)_2{\cdot}4H_2O$), and molybdenum chloride ($MoCl_5$). Hydrochloric acid (HCl), concentrated sulfuric acid (H_2SO_4), ethanol (C_2H_5OH), N-Dimethyl formamide (DMF), hydrogen peroxide (H_2O_2), ethylenediamine (EDA,$C_2H_8N_2$), and thioacetamide (CH_3CSNH_2) are among the solvents used (Sun et al., 2023; Yin et al., 2023; Govindaraju et al., 2020; He et al., 2018).

Other methods include

Colloidal Synthesis

This method creates small particles of colloidal substance. In aqueous or non-aqueous solutions, surfactants and other additives such as pH modifiers and stabilizers are typically added to precursor species. Also, heating, agitation, or inert atmospheres may also be used. For precise control over the properties of nanostructures, colloidal synthesis offers flexibility in adjusting parameters including temperature, time, solvent system, precursors, concentration, and surfactants. This enables controlled synthesis with mono-dispersity, uniform size and shape (Tan et al., 2018).

Microwave Synthesis

Microwave irradiation facilitates rapid and energy-efficient heating of reactants, promoting close interaction among various components (Mehta et al., 2024). Compared to traditional heating techniques, this approach is more environmentally friendly and avoids agglomeration during preparation (Liu et al.,2014). The microwave-assisted method works well for creating nanocomposites, like those made of graphene and TMDs. Among the many benefits of the microwave-assisted approach are quick heating, a shorter synthesis time, great energy efficiency, good synthesis control, and an eco-friendly reaction process. It is evident that these benefits outweigh those of conventional heating techniques (Wang et al., 2016;Wang et al.,2022).

Additive Manufacturing of TMDs

Additive manufacturing, also known as 3D printing is a manufacturing technique that enables the layer-by-layer creation of 3D objects based on a digital model or design. Complex designs may now be quickly customized and fabricated which are sometimes impractical or unfeasible using traditional production methods (Ambrosi et al., 2020).

Lithography Techniques

The science of surface patterning is known as lithography. Lithography methods are used to precisely nanofabricate patterned electrodes for water electrolysis and to improve comprehension of the links between structure, composition, and activity. There are numerous lithography techniques that enable surface patterning with resolutions ranging from the nanoscale (10 nm) to the macroscale (~1 mm). Based on their operational principles, the various lithography techniques can be roughly categorized as pattern transfer, self-assembly, and direct write approaches (Mehla, 2022).

Challenges and Future Directions

Even though electrocatalysis has advanced significantly in the recent years, there are still a number of issues that need to be resolved before these technologies can be widely used in real-world applications (Mehta et al., 2024), such as low electrical conductivities and exchange current densities, high overpotentials which subsequently lead to poor yields of the overall hydrogen. However, despite the intriguing and excellent properties of TMD-based electrocatalysts toward the HER process, the efficiency of sustainable hydrogen production is still limited and faces a number of obstacles that include poor scalable synthesis of the TMD-based electrocatalysts, restricted researches on the TMD-based electrocatalysts family, non-reactivity of their basal plane which results in the low catalytic activity, etc.

Therefore, to greatly resolve some of these challenges several methods of increasing catalytic activities, including heteroatom doping, the formation of janus TMDs, the construction of heterostructures, phase engineering, and nanostructuring, must be used in order to address the issue of the low catalytic performance of the reported TMDs-based electrocatalysts. It is also very imperative that the different processes for producing TMD-based electrocatalysts be improved. Furthermore, to fully utilize the potential of other members of the TMD-based family in the electrocatalysis field, more researches are required. Thus, future studies can concentrate on using and utilizing theoretical modeling, such as hybrid techniques that combine machine learning and density functional theory (DFT), in the design and discovery of novel TMD-based electrocatalysts.

CONCLUSION

The paper presented a review on the application of TMD-based electrocatalysts in electrocatalytic water splitting. Brief overviews of TMDs, their structural and electronic properties were discussed in the first place. However, the paper delved into the concept of electrocatalytic water splitting with clear explanations on the two half reactions that constituted the entire process: HER and OER. The fact that the sole aim is to improve and develop new electrocatalyst materials that are cheaper and earth-abundant; some important descriptors of a good electrocatalyst were elaborated. Not only that, the strategies of enhancing the catalytic activity of the reported TMD-based electrocatalysts were highlighted, such as doping, formation of Janus TMDs, and formation of heterostructures. Close to the end, the review examined some of the methods of synthesizing and preparing the TMDs-based electrocatalysts. Finally, the problems limiting the progress of the field as well as solutions to some of them were discussed. The primary goal is to have TMD-based electrocatalysts with comparable catalytic activities to that of Pt groups, and achieving this will undoubtedly revolutionize the entire field, leading to effective production of green hydrogen.

REFERENCES

Ambrosi, A., Shi, R.R.S. and Webster, R.D. (2020). 3D-printing for electrolytic processes and electrochemical flow systems. *Journal of Materials Chemistry A,8 (42),* 21902-21929.

Ataca, C., Şahin, H. and Ciraci, S. (2012). Stable, Single-Layer MX_2 Transition-Metal Oxides and Dichalcogenides in a Honeycomb-Like Structure. *Journal of Physical Chemistry C,116(16)*, 8983-8999.

Baig, N., Kammakakam, I. and Falath, W. (2021). Nanomaterials: a review of synthesis methods, properties, recent progress, and challenges. *Materials Advances, 2,*1821-1871.

Bonde, J., Moses, P.G., Jaramillo, T. F., Nørskov, J. K. and Chorkendorff I. (2009). Hydrogen evolution on nano-particulate transition metal sulfides. *Faraday Discussion, 140,* 219-231.

Cao, X., Tang, Y., Duus, J. Ø., and Chi, Q. (2019). Engineering two-dimensional transition metal dichalcogenide electrocatalysts for water splitting hydrogen generation. In HANDBOOK OF ECOMATERIALS,1845-1873, Springer. https://doi.org/10.1007/978-3-319-68255-6_174

Chen, Y., Yang, K., Jiang, B., Li, J., Zeng, M. and Fu, L., (2017). Emerging two-dimensional nanomaterials for electrochemical hydrogen evolution. *Journal of Material Chemistry A, 5*, 8187-8208.

Chen, Z., Cummins, D., Reinecke, B. N., Clark, E., Sunkara, M. K., Jaramillo, T. F. (2011). Core-shell MoO_3-MoS2 Nanowires for Hydrogen Evolution: A Functional Design for Electrocatalytic Materials. *Nano Letters, 11,* 4168−4175.

Chen, X., Wang, Z., Qiu, Y., Zhang, J., Liu, G., Zheng, W., et al. (2016). Controlled growth of vertical 3D MoS2(1− x) Se_{2x} nanosheets for an efficient and stable hydrogen evolution reaction. *Journal of Materials Chemistry A, 4,* 18060-18066.

Chhowalla, M., Shin, H.S., Eda, G., Li, L.J., Loh, KP. and Zhang, H. (2013). The chemistry of two-dimensional layered transition metal dichalcogenide nanosheets. *Nature Chemistry,5*, 263–275. https://doi.org/10.1038/nchem.1589.

Chia, X., Ambrosi, A., Lazar, P., Sofer, Z., Pumera, M. (2016). Electrocatalysis of layered Group 5 metallic transition metal dichalcogenides (MX_2, M = V, Nb, and Ta; X = S, Se, and Te). *Journal of Materials Chemistry A, 4(37),* 14241-14253.

Dang, L. N., Liang, H. F., Zhuo, J. Q., Lamb, B. K., Sheng, H. Y., Yang, Y. and Jin, S. (2018). Direct synthesis and anion exchange of noncarbonate-intercalated NiFe-layered double hydroxides and the influence on electrocatalysis. *Chemistry of Materials, 30(13),* 4321–4330. https://doi.org10.1021/acs.chemmater.8b01334.

Dhand, C., Dwivedi, N., Loh, X.J., Ying, ANJ., Verma, N.K., Beuerman, R.W, et al. (2015). Methods and strategies for the synthesis of diverse nanoparticles and their applications: a comprehensive overview. *RSC Advances,5(127),* 105003-105037.

Ding, Q., Song, B., Xu, P. and Jin S. (2016). Efficient electrocatalytic and photoelectrochemical hydrogen generation using MoS_2 and related compounds. *Chem, 1(5),* 699-726.

Ding, Y., Wang, Y., Ni, J., Shi, L., Shi, S., Tang, W. (2011). First principles study of structural, vibrational and electronic properties of graphene-like MX_2 (M=Mo, Nb, W, Ta; X=S, Se, Te) monolayers. *Physica B, 406(11),* 2254-2260.

Ding, Q., Zhai, J., Cabán-Acevedo, M., Shearer, M. J., Li, L., Chang, H.-C., Tsai, M.-L., Ma, D., Zhang, X., Hamers, R. J., He, J.-H. and Jin, S. (2015). Designing efficient solar-driven hydrogen evolution photocathodes using semitransparent MoQxCly (Q = S, Se) catalysts on Si micropyramids. *Advanced Materials, 27(41),* 6511-6518.

Dong, Y., Dang, J., Wang, W., Yin, S. and Wang, Y. (2018). First-principles determination of active sites of Ni metal-based electrocatalysts for hydrogen evolution reaction. *ACS Applied Materials and Interfaces, 10(46),* 39624–39630.

Dresselhaus, M. S. and Thomas, I. L. (2001). Alternative energy technologies. *Nature, 414*, 332-337.

Dresp, S., Dionigi, F., Klingenhof, M. and Strasser, P. (2019). Direct electrolytic splitting of seawater: opportunities and challenges. *ACS Energy Letters,4(4),* 933–942.

Er, D., Ye, H., Frey, N.C., Kumar, H., Lou, J. and Shenoy, V.B. (2018). Prediction of enhanced catalytic activity for hydrogen evolution reaction in janus transition metal dichalcogenides. *Nano Letters, 18(6)*, 3943-3949. https://doi.org/10.1021/acs.nanolett.8b01335.

Faber, M. S. and Jin, S. (2014). Earth-abundant inorganic electrocatalysts and their nanostructures for energy conversion applications. *Energy and Environmental Sciences,7(11),* 3519-3542.

Faber, M. S., Lukowski, M. A., Ding, Q., Kaiser, N. S., Jin, S. (2014). *Journal of Physical Chemistry C,118(37),* 21347–21356.

Faid, A.Y., A. Barnett, O., Seland, F. and Sunde, S. (2021). NiCu mixed metal oxide catalyst for alkaline hydrogen evolution in anion exchange membrane water electrolysis. *Electrochimica. Acta, 371(12),* 137837. http://dx.doi.org/10.1016/j.electacta.2021.137837

Fu, Q., Yang, L., Wang, W., Han, A., Huang, J., Du, P., Fan, Z., Zhang, J. and Xiang, B. (2015). Synthesis and enhanced electrochemical catalytic performance of monolayer WS2(1–x)Se2x with a tunable band gap. *Advanced Materials, 27,* 4732-4738.

Fu, Q., Han, J., Wang, X., Xu, P., Yao, T., Zhong, J., Zhong, W., Liu, S., Gao, T., Zhang, Z., Xu, L. and Song, B. (2020). 2D transition metal dichalcogenides: Design, modulation, and challenges in electrocatalysis. *Advanced Materials*, 1907818. https://doi.org/10.1002/adma.201907818.

Gao, G., Sun, Q. and Du, A. (2016). Activating catalytic inert basal plane of molybdenum disulfide to optimize hydrogen evolution activity via defect doping and strain engineering. *Journal of Physical Chemistry C, 120*, 16761−16766.

Gao, M.R., Chan, M. and Sun, Y. (2015). Edge-terminated molybdenum disulfide with a 9.4-Å interlayer spacing for electrochemical hydrogen production. *Nature Communications* 6, 7493. https://doi.org/10.1038/ncomms8493

Ghorbani-Asl, M., Enyashin, A.N., Kuc, A., Seifert, G. and Heine, T. (2013). Defect-induced conductivity anisotropy in MoS_2 monolayers. *Physical Review B, 88,* 245440. https://doi.org/10.1103/PhysRevB.88.245440

Gholamvand, Z., McAteer, D., Backes, C., McEvoy, N., Harvey, A., Berner, N.C., Hanlon, D., C. Bradley, I., Godwin, A., Rovetta, M. E., Lyons, G., Duesberg, G. S. and Coleman, J. N. (2016). Comparison of liquid exfoliated transition metal dichalcogenides reveals $MoSe_2$ to be the most effective hydrogen evolution catalyst. *Nanoscale, 8*, 5737-5749.

Gileadi, E. and Kirowa-Eisner, E. (2005). Concerning the Tafel equation and its relevance to charge transfer in corrosion. *Corrosion Science, 47,(12)*, 3068-3085.

Giuffredi G., Asset T., Liu Y., Atanassov P., and Di Fonzo F. (2021).Transition metal chalcogenides as a versatile and tunable platform for catalytic CO_2 and N_2 electroreduction. *ACS Materials Au,1*, 6−36.

Govindaraju, V.R., Sreeramareddygari, M., Hanumantharayudu, N.D., Devaramani S., Thippeswamy, R., Surareungchai, WJEP, et al. (2020). Solvothermal decoration of Cu_3SnS_4 on reduced graphene oxide for enhanced electrocatalytic hydrogen evolution reaction. *Environmental progress and sustainable energy*, e13558. https://doi.org/10.1002/ep.13558.

Guo, C., Jiao, Y., Zheng, Y., Luo, J., Davey, K. and Qiao, S.-Z. (2019). Intermediate modulation on noble metal hybridized to 2D metal-organic framework for accelerated water electrocatalysis. *Chem,5*, 2429-2441.

Han, S. A, Bhatia, R. and Kim S.-W. (2015). Synthesis, properties and potential applications of two-dimensional transition metal dichalcogenides. *Nano Convergence, 2*,17. https://doi.org/10.1186/s40580-015-0048-4

He, H.-Y., He, Z. and Shen Q. (2021). Novel assembly of Janus RGO/1T-SeMoS nanosheets structures showing high-efficient electrocatalytic activity for hydrogen evolution. *Colloids and Interface Science Communications, 45(17):*100509. http://dx.doi.org/10.1016/j.colcom.2021.100509

He, Q., Wan, Y., Jiang, H., Wu, C., Sun Z., Chen, S., et al. (2018). High-metallic-phase-concentration $Mo_{1-x}W_xS_2$ nanosheets with expanded interlayers as efficient electrocatalysts. *Nano research,11*,1687–1698. https://doi.org/10.1007/s12274-017-1786-x

Henckel, D. A., Lenz, O. M., Krishnan, K. M. and Cossairt, B. M. (2018). Improved HER catalysis through facile, aqueous electrochemical activation of nanoscale WSe_2. *Nano Letters*, *18,* 2329-2335.

Hernandez Ruiz, K., Wang, Z., Ciprian, M., Zhu, M., Tu, R., Zhang, L, et al. (2022). Chemical vapor deposition mediated phase engineering for 2D transition metal dichalcogenides: strategies and applications. *Small science, 2(1),* 2100047. http://dx.doi.org/10.1002/smsc.202100047

Hoegh-Guldberg, O., Mumby, P. J., Hooten, A. J., R. S. Steneck, P. Greenfield, E. Gomez, C. D. Harvell, P. F. Sale, A. J. Edwards, K. Caldeira, N. Knowlton, C. M. Eakin, R. Iglesias-Prieto, Muthiga, N., Bradbury, R. H., Dubi, A., Hatzioloset, M. E. al., (2007). Coral reefs under

rapid climate change and ocean acidification. *Science, 318(5857),* 1737-1742.

Huang, W., Zhou, D., Qi, G. and Liu X. (2021). Fe-doped MoS2 nanosheets array for high-current-density seawater electrolysis. *Nanotechnology, 32*, 415403. https://doi.org/10.1088/1361-6528/ac1195

Huang, H., Hu, G., Hu, C. and Fan, X. (2022). Enhanced hydrogen evolution reactivity of T'-phase tungsten dichalcogenides (WS_2, WSe_2, and WTe_2) Materials: A DFT Study. *International Journal of Molecular Sciences, 23*, 11727. https://doi.org/10.3390/ijms231911727.

Huang, W. and Li, W.-X. (2019). Surface and interface design for heterogeneous catalysis. *Physical Chemistry Chemical Physics, 21*, 523–536.

Idrees, M., Din, H.U., Rehman, S.U., Shafiq, M., Saeed, Y., Bui, H.D., Nguyen, C.V. and Amin B. (2020). Electronic properties and enhanced photocatalytic performance of van der Waals heterostructures of ZnO and Janus transition metal dichalcogenides. *Physical Chemistry Chemical Physics, 22*,10351.

Jaberi S.Y.S., Ghaffarinejad A. and Khajehsaeidi Z. (2021). The effect of annealing temperature, reaction time, and cobalt precursor on the structural properties and catalytic performance of CoS_2 for hydrogen evolution reaction. *Internal Journal of Hydrogen Energy, 46*, 3922.

Jaramillo, T. F., Jørgensen, K. P., Bonde, J., Nielsen, J. H., Horch, S. and Chorkendorff, I. (2007). Identification of active edge sites for electrochemical H_2 evolution from MoS_2 nanocatalysts. *Science, 317*, 100−102.

Jiao, Y., Zheng, Y., Jaroniec, M. and Qiao, S. Z. (2015). Design of electrocatalysts for oxygen- and hydrogen-involving energy conversion reactions. *Chemical Society Review, 44*, 2060.

Jiang A., Zhang, B., Li, Z., Jin, G. and Hao, J. (2018). Vanadium-Doped WS_2 Nanosheets Grown on Carbon Cloth as a Highly Efficient Electrocatalyst for the Hydrogen Evolution Reaction. *Chemistry- an Asian Journal, 13(11),* 1438-1446.

Ji, Y., Yang, M.,Lin, H., Hou, T., Wang, L., Li, Y. and Lee, S.-T. (2018). Janus structures of transition metal dichalcogenides as the heterojunction photocatalysts for water splitting. *Journal of Physical Chemistry C, 122,* 3123.

Kam, K.K. and Parkinson, B.A. (1982). Detailed photocurrent spectroscopy of the semiconducting group VIB transition metal dichalcogenides. *Journal of Physical Chemistry, 86(4),* 463-467.

Kaur, S.P. and Kumar, T. J. D. (2021). Tuning structure, electronic, and catalytic properties of non-metal atom doped Janus transition metal dichalcogenides for hydrogen evolution. *Applied Surface Science,552,* 149146.

Kheibar D., Neda S., Fereshteh A., Bahar S., Aida, M., Sana, S.-A., Rouholah, Z.-D. (2023). Metal chalcofenides for sensing applications. *Fundamental of sensor technology,* 551-589.

Kibsgaard, J., Chen, Z., Reinecke, B. N., Jaramillo, T. F. (2012). Engineering the surface structure of MoS_2 to preferentially expose active edge sites for electrocatalysis. *Nature Materials,11,* 963−969.

Koper, M. T. M. (2013). Theory of multiple proton–electron transfer reactions and its implications for electrocatalysis. *Chemical Science, 4*, 2710-2723.

Kuc, A., Zibouche, N. and Heine, T. (2011). Covering condensed matter and materials physics influence of quantum confinement on the electronic structure of the transition metal sulfide. *Physical Review B: Condensed Matter, 83*, 245213.

Kuc, A., Heine, T. and Kis, A. (2015). Electronic properties of transition-metal dichalcogenides. *Material Research Society, 40,* 577-584. DOI: 10.1557/mrs.2015.143

Kunhiraman, A., Bradha, K.M. and Rakkesh R. A. (2021). Nickel-doped two-dimensional molybdenum disulfide for electrochemical hydrogen evolution reaction. *Journal of Material Research, 36,* 4141.

Li, Y., Abbott, J., Sun, Y., Sun, J., Du, Y., Han, X., Wu, G. and Xu, P. (2019). Ru nanoassembly catalysts for hydrogen evolution and oxidation reactions in electrolytes at various pH values. *Applied Catalysts B, 258*, 117952.

Li, J., Liu, P., Qu, Y., Liao, T. and Xiang, B. (2018). WSe2/rGO hybrid structure: A stable and efficient catalyst for hydrogen evolution reaction. *International Journal of Hydrogen Energy, 43*, 2601-2609.

Li, L., Qin, Z., Ries L., Hong S., Michel, T., Yang J., Salameh, C., Bechelany, M., Miele, P., Kaplan, D., Chhowalla, M. and Voiry, D. (2019). Role of sulfur vacancies and undercoordinated Mo regions in MoS_2 nanosheets toward the evolution of hydrogen. ACS

Nano. 13(6),6824-6834. https://doi.org/10.1021/acsnano.9b01583.

Li, Y., Wang, H., Xie, L., Liang, Y., Hong, G. and Dai, H. (2011). MoS_2 nanoparticles grown on graphene: An advanced catalyst for the hydrogen evolution reaction. *Journal of American Chemical Society, 133,* 7296− 7299.

Li, T. and Galli, G. (2007). Electronic properties of MoS_2 nanoparticles. *Journal of Physical Chemistry C, 111*, 16192-16196.

Li, F. and Xue, M. (2016). Two-dimensional transition metal dichalcogenides for electrocatalytic energy conversion applications. InTech. doi:10.5772/63947.

Li, H., Tan Y., Liu, P., Guo, C., Luo, M., Han, J., Lin, T., Huang, F. and Chen, M. (2016). Atomic-sized pores enhanced electrocatalysis of TaS_2 nanosheets for hydrogen evolution. *Advanced Materials, 28*, 8945-8949.

Li, R., Yang, L., Xiong, T., Wu, Y., Cao, L., Yuan D. and Zhou, W. (2017). Nitrogen doped MoS_2 nanosheets synthesized via a low-temperature process as electrocatalysts with enhanced activity for hydrogen evolution reaction. *Journal of Power Sources, 356*, 133.

Li, H., Tsai, C., Koh, A. L., Cai, L., Contryman, A. W., Fragapane, A. H., Zhao, J., Han, H. S., Manoharan, H. C., Abild-Pedersen F., Nørskov J. K. and Zheng, X. (2016). Activating and optimizing MoS_2 basal planes for hydrogen evolution through the formation of strained sulphur vacancies. *Nature Materials, 15,* 48-53.

Liang, J., Ma, F., Hwang, S., Wang, X., Sokolowski, J., Li, Q., Wu, G. and Su, D. (2019). Atomic arrangement engineering of metallic nanocrystals for energy-conversion electrocatalysis. *Joule, 3,* 956-991.

Lin, J., Peng, Z., Wang, G., Zakhidov, D., Larios, E., Yacaman, M.J. and Tour, J. M. (2014). Enhanced electrocatalysis for hydrogen evolution reactions from WS_2 nanoribbons. *Advanced Energy Materials, 4,* 1301875.

Lin L., Fu, Q., Han, Y., Wang, J., Zhang, X., Zhang, Y., Hu, C., Liu, Z., Sui, Y. and Wang, X. (2019). Fe doped skutterudite-type CoP_3 nanoneedles as efficient electrocatalysts for hydrogen and oxygen evolution in alkaline media. *Journal of Alloys and Compounds, 808*, 151767.

Lin, L., Sherrell, P., Liu, Y., Lei, W., Zhang, S., Zhang, H., Wallace, G.G. and Chen, J. (2020). Engineered 2D transition metal dichalcogenides-a vision of viable hydrogen evolution reaction catalysis. *Advanced Energy Materials, 10,* 1903870.

Liu, Y., Wu, J., Hackenberg, K.P., Zhang, J., Wang, Y.M., Yang, Y., Keyshar, K., Gu, J., Ogitsu, T., Vajtai, R., et al. (2017). Self-optimizing, highly surface active layered metal dichalcogenide catalysts for hydrogen evolution. *Nature Energy, 2*, 17127. https://doi.org/10.1038/nenergy.2017.127.

Liu, J.X., Yin, H.J., Liu, P.R., Chen, S., Yin, S.W., Wang, W.L., Zhao, H.J. and Wang, Y. (2019). Theoretical understanding of electrocatalytic hydrogen production performance by low-dimensional metal-organic frameworks on the basis of resonant charge-transfer mechanisms. *Journal of Physical Chemical Letters, 10*, 6955–6961.

Liu, L., Kumar, S.B., Ouyang, Y. and Guo, J. (2011). Performance limits of monolayer transition metal dichalcogenide transistors. *In IEEE Transactions on Electron Devices, 58(9),* 3042-3047, https://doi.org/10.1109/TED.2011.2159221.

Liu, Y., Hua, X., Xiao, C., Zhou, T., Huang, P., Guo, Z., Pan, B. and Xie, Y. (2016). Heterogeneous Spin States in Ultrathin Nanosheets Induce Subtle Lattice Distortion To Trigger Efficient Hydrogen Evolution. *Journal of American Chemical Society, 138(15),* 5087-5092. https://doi.org/10.1021/jacs.6b00858.

Liu, N., Wang, X., Xu, W., Hu, H., Liang, J. and Qiu, J.J.F. (2014). Microwave-assisted synthesis of MoS_2/graphene nanocomposites for efficient hydrodesulfurization, 119, 163–169.

Lukowski, M.A., Daniel, A.S., Meng, F., Forticaux, A., Li, L. and Jin, S. (2013). Enhanced hydrogen evolution catalysis from chemically exfoliated metallic MoS_2 nanosheets. *Journal of American Chemical Socety, 135,* 10274−10277.

Lv, X.-J, She, G.-W., Zhou, S.-X. and Li, Y.-M. (2013). Highly efficient electrocatalytic hydrogen production by nickel promoted molybdenum sulfide microspheres catalysts. RSC Advances, 3(44), 21231-21236.

Mak, K.F., Lee, C., Hone, J., Shan, J. and Heinz, T.F. (2010). Atomically thin MoS_2: a new directgap semiconductor. *Physical Review Letters, 105,* 136805. https://doi.org/10.1103/PhysRevLett.105.136805.

Manzeli, S., Ovchinnikov D., Pasquier, D., Yazyev, O.V. and Kis, A. (2017). 2D transition metal dichalcogenides. Nature Review Materials, 2, 17033

McCrum, I.T. and Koper, M.T. (2020). The role of adsorbed hydroxide in hydrogen evolution reaction kinetics on modified platinum. *Nature Energy, Nature, 5(11),* 891-899.

Mehla, S. (2022). Design and fabrication of gold microelectrode arrays for SERS-based chemical sensing. Melbourne: RMIT University.

Mehta S., Thakur, R., Rani S., Nagaraja, B.M., Mehla, S. and Kainthla, I. (2024) Recent advances in ternary transition metal dichalcogenides for electrocatalytic hydrogen evolution reaction. *International Journal of Hydrogen Energy*, 82, 1061–1080.

Najafi, L., Bellani, S., Oropesa-Nuñez, R., Ansaldo, A., Prato, M., Del Rio Castillo, A.E. and Bonaccorso, F. (2018). Doped-$MoSe_2$ nanoflakes/3d metal oxide–hydr(Oxy)oxides hybrid catalysts for pH-universal electrochemical hydrogen evolution reaction. *Advanced Energy Material, 8,* 1801764.

Naz, R., Liu, Q., Abbas, W., Imtiaz, M., Zada, I., Ahmad, J., et al. (2019). One-pot hydrothermal synthesis of ternary 1T-MoS_2/hexa-WO_3/graphene composites for high-performance supercapacitors. *Chemistry- a European Journal, 25*,16054–16062.

Nørskov, J.K., Bligaard, T., Logadottir, A., Kitchin, J., Chen, J.G., Pandelov, S., Stimming, U. (2005). Trends in the exchange current for hydrogen evolution. Jornal of Electrochemical Society,152, J23.

Ogunkunle, S. A., Bouzid, A., Hinsch, J.J., Allen, O.J., White, J.J., Bernard, S., Wu, Z., Zhu, Y. and Wang, Y. (2024). Defect engineering of 1T′ MX_2 (M = Mo, W and X = S, Se) transition metal dichalcogenide-based electrocatalyst for alkaline hydrogen evolution reaction. Journal of Physics: Condensed Matter, 36, 145002.

Ouyang, Y., Ling, C., Chen, Q., Wang, Z., Shi, L. and Wang, J. (2016). Activating Inert Basal planes of MoS_2 for hydrogen evolution reaction through the formation of different Intrinsic defects. Chemistry of Materials, 28, 4390−4396.

Paez-Ornelas, J. I., Ponce-Pérez, R., Fernández-Escamilla, H. N., Hoat, D. M., Murillo-Bracamontes E. A., Moreno-Armenta M.G., Donald H.G., and Guerrero-Sánchez, J. (2021). The effect of shape and size in the stability of triangular Janus MoSSe quantum dots. Scientific Reports, 11, 21061. doi:10.1038/s41598-021-00287-6.

Polvani L. M., Previdi, M., England, M., Chiodo, R.G. and Smith K. L. (2020). Substantial twentieth-century Arctic warming caused by ozone-depleting substances. Nature Climate Change, 10, 130-133.

Prabhu, P., Jose, V. and Lee, J.-M. (2020). Design strategies for development of TMD-based heterostructures in electrochemical energy systems. *Matter, 2(3),* 526–553.

Ramki, S., Sukanya, R., Chen, S.-M., Sakthivel, M., and Wang, J. Y., (2019). Simple hydrothermal synthesis of defective $CeMoSe_2$ dendrites as an effective electrocatalyst for the electrochemical sensing of 4-nitrophenol in water samples. *New Journal of. Chemistry, 43*, 17200.

Sakthivel, M, Ramaraj, S., Chen, S.-M., Chen, T.-W. and Ho, K. (2019). Transition-metal-doped molybdenum diselenides with defects and abundant active sites for efficient performances of enzymatic biofuel cell and supercapacitor applications. Interfaces, 11, 18483–18493.

Shen, J., Ji, J., Dong, P., Baines, R., Zhang, Z., Ajayan, P.M., et al. (2016). Novel $FeNi_2S_4$/TMD-based ternary composites for supercapacitor applications. Journal of Materials Chemistry A, 4(22), 8844–8850.

Shifa, T.A., Wang, F., Liu, K., Xu, K., Wang, Z., Zhan, X., et al. (2016). Engineering the electronic structure of 2D WS_2 nanosheets using Co incorporation as $Co_xW_{(1-x)}S_2$ for conspicuously enhanced hydrogen generation. Small, 12, 3802–3809.

Shi, Y., Zhou, Y., Yang, D.R., Xu, W.X., Wang, C., Wang, F.B., Xu, J.J., Xia, X.H. and Chen, H.Y. (2017). Energy level engineering of MoS_2 by transition-metal doping for accelerating hydrogen evolution reaction. Journal of American Chemical Society, 139(43), 15479-15485. https://doi.org/10.1021/jacs.7b08881.

Shi, H., Zhang, H., Li, M., Wang, Y. and Wang, D. (2021). Nanoflower-like 1T/2H mixedphase $MoSe_2$ as an efficient electrocatalyst for hydrogen evolution. Journal of Alloys and Compound, 878, 160381.

Shim, G.W., Hong, W., Yang, S.Y. and Choi, S. (2017). Tuning the catalytic functionality of transition metal dichalcogenides grown by chemical vapour deposition. Journal of Materials Chemistry A, 5,14950–14968.

Sim, Y., Chae, Y. and Kwon, S.-Y. (2022). Recent advances in metallic transition metal dichalcogenides as electrocatalysts for hydrogen evolution reaction. iScience, 25, 105098.

Sk´ulason, E., Tripkovic, V., Bjo¨rketun, M.E., Gudmundsdóttir, S., Karlberg, G., Rossmeisl, J., Bligaard, T., Jónsson, H. and Nørskov, J.K. (2010). Modeling the electrochemical hydrogen oxidation and evolution reactions on the basis of density functional theory calculations. Journal of Physical Chemistry C, 114, 18182–18197.

Splendiani, A., Sun, L., Zhang, Y., Li, T., Kim, J., Chim, C.-Y., Galli, G., and Wang, F. (2010). Emerging photoluminescence in monolayer MoS_2. Nano Letters, 10, 1271–1275. https://doi.org/10.1021/nl903868w.

Sukanya R., Barwa T. N., Luo Y., Dempsey E., and Breslin C.B. (2022). Emerging layered materials and their applications in the corrosion protection of metals and alloys. Sustainability, 14(7), 4079. https://doi.org/10.3390/su14074079

Sukanya, R., da Silva Alves, D.C. and Breslin, C.B. (2022). Recent developments in the applications of 2D transition metal dichalcogenides as electrocatalysts in the generation of hydrogen for renewable energy conversion. *Journal of The Electrochemical Society*, 169, 064504.

Sun, L., Gao, M., Jing, Z., Cheng, Z., Zheng, D., Xu, H., Zhou, Q. and Lin J. (2022). 1T phase enriched P doped WS_2 nanosphere for highly efficient electrochemical hydrogen evolution reaction. Chemical Engineering Journal, 429, 132187. https://ui.adsabs.harvard.edu/link_gateway/2022ChEnJ.42932187S/doi:10.1016/j.cej.2021.132187.

Sun, X., Dai, J., Guo, Y., Wu, C., Hu, F., Zhao, J., Zeng, X. and Xie, Y. (2014). Semimetallic molybdenum disulfide ultrathin nanosheets as an efficient electrocatalyst for hydrogen evolution. Nanoscale, 6, 8359-8367.

Sun, Y., Wang, B., Liu, X., Gao, L. and Shangguan, W.J.C. (2023). Synthesis of ternary cross-linked MoS2/WS2/CdS photocatalysts for photocatalytic H_2 production. Catalyst,13,1149. https://doi.org/10.3390/catal13081149.

Tan, C., Chen, J., Wu, X.-J., Zhang H (2018). Of hybrid nanostructures. *Nature Reviews Materials 3(2)*, 17089. https://doi.org/10.1038/natrevmats.2017.89

Tang, Q. and Jiang, D.-E. (2016). Mechanism of hydrogen evolution reaction on 1T- MoS_2 from first principles. *ACS Catalyst*, 6, 4953.

Tanwar, S., Arya, A., Gaur, A. and Sharma, A.L. (2021). Transition metal dichalcogenide (TMDs) electrodes for supercapacitors: a comprehensive review. *Journal of Physics: Condensed Matter, 33(30).* https://doi.org/10.1088/1361-648X/abfb3c.

Tian, X., Zhao, P. and Sheng,W. (2019). Hydrogen evolution and oxidation: mechanistic studies and material advances. *Advanced Materials, 31*, 1808066.

Tongay, S., Suh, J., Ataca, C., Fan, W., Luce, A., Kang, J.S., Liu, J., Ko C., Raghunathanan R., Zhou J., Ogletree F., J. Li , Grossman J.C. and Wu J. (2013). Defects activated photoluminescence in two-dimensional semiconductors:interplay between bound, charged,

and free excitons. *Scientific Report, 3*, 2657.

Turner, J. A. (2004). Sustainable hydrogen production. *Science, 305*, 972.

Tsai, C., Li, H., Park, S., Park, J., Han, H. S., Nørskov, J. K., Zheng, X. and Abild-Pedersen, F. (2017). Electrochemical generation of sulfur vacancies in the basal plane of MoS_2 for hydrogen evolution. Nature Communications, 8, 15113.

Vikraman, D., Hussain, S., Patil, S. A., Truong, L., Arbab, A. A., Jeong, S. H., Chun, S.- H., Jung J. and Kim, H.-S. (2021). Engineering $MoSe_2/WS_2$ hybrids to replace the scarce platinum electrode for hydrogen evolution reactions and dye-sensitized solar cells. ACS Applied Material Interfaces,13,5061.

Vikraman, D., Hussain, S., Karuppasamy, K., Kathalingam, A., Jo, E.-B., Sanmugam, A., Jung, J. and Kim, H.-S. (2022). Engineering the active sites tuned MoS_2 nanoarray structures by transition metal doping for hydrogen evolution and supercapacitor applications. Journal of Alloys and Compound,893,162271.

Voiry, D., Salehi, M., Silva, R., Fujita, T., Chen, M., Asefa, T., Shenoy, V.B., Eda, G. and Chhowalla, M. (2013). Conducting MoS_2 nanosheets as catalysts for hydrogen evolution reaction. Nano Letters,13, 6222.

Wang, P., Zhang, X., Zhang, J., Wan, S., Guo, S., Lu, G., Yao, J. and Huang, X. (2017). Precise tuning in platinum-nickel/nickel sulfide interface nanowires for synergistic hydrogen evolution catalysis. Nature Communications, 8, 14580.

Wang, J., Shu, H., Zhao, T., Liang, P., Wang, N., Cao, D. and Chen, X. (2018). Intriguing electronic and optical properties of two-dimensional Janus transition metal dichalcogenides. Physical Chemistry Chemical Physics,20,18571.

Wang, R., Li, X., Gao, T., Yao, T., Liu, S., Wang, X., Han, J., Zhang, P., Cao, X., Zhang, X., Zhang, Y. and Song, B. (2019). Beyond 1T-phase synergistic electronic structure and defects engineering in 2H-MoS2xSe2(1-x) nanosheets for enhanced hydrogen evolution reaction and sodium storage. ChemCatChem, 11, 3200-3211.

Wang, J., Wang, W., Wang, Z., Chen, J. G. and Liu, C.-j. (2016). Porous MS_2/MO_2 (M = W, Mo) nanorods as efficient hydrogen evolution reaction catalysts. ACS Catalysts, 6, 6585−6590.

Wang, M., Wang, X., Zheng, M. and Zhou, X. (2022). Improved catalytic activity of "Janus" MoSSe based on surface interface regulation. *Molecules, 27(18),* 6038.

Wang, Z., Zhao, C., Gui, R., Jin, H., Xia, J., Zhang, F., et al. (2016). Synthetic methods and potential applications of transition metal dichalcogenide/graphene nanocomposites. *Coordination Chemistry Reviews, 326*, 86–110.

Wang, J., Wu, W., Kondo, H., Fan, T. and Zhou, H. (2022). Recent progress in microwave-assisted preparations of 2D materials and catalysis applications. *Nanotechnology, 33*,342002.

Wazir, M.B., Daud, M., Safeer, S., Almarzooqi, F. and Qurashi, A. (2022). Review on 2D molybdenum diselenide ($MoSe_2$) and its hybrids for green hydrogen (H_2) generation applications. *ACS Omega, 7*, 16856–16865. https://doi.org/10. 1021/acsomega.2c00330.

Wei, J., Zhou, M., Long, A., Xue, Y., Liao, H., Wei, C. and Xu, Z.J. (2018). Heterostructured electrocatalysts for hydrogen evolution reaction under alkaline conditions. *Nanomicro Letters, 10(4)*,75. doi:10.1007/s40820-018-0229-x.

Wilson, J.A., Di Salvo, F.J. and Mahajan, S. (1974). Charge-density waves in metallic, layered, transition-metal dichalcogenides. *Physical Review Letters,32,* 882–885. https://doi.org/10.1103/PhysRevLett.32.882.

Wu, H., Zuo, X., Wang, S.P., Yin, J.W., Zhang, Y.N. and Chen, J. (2019). Theoretical and experimental design of Pt-$Co(OH)_2$ electrocatalyst for efficient HER performance in alkaline solution. *Progress in Natural Science: Materials International, 29,* 356–361.

Wu, L. and Hofmann, J.P. (2021). Comparing the intrinsic HER activity of transition metal dichalcogenides: pitfalls and suggestions. ACS Energy Letters, 6, 2619–2625.

Xiong, Q., Wang, Y., Liu, P.-F., Zheng L.-R., Wang G., Yang H.-G., Wong P.-K., Zhang, H. and Zhao H. (2018). Cobalt covalent doping in MoS_2 to induce bifunctionality of overall water splitting. *Advanced Materials, 30,* 1801450.

Xiong Q., Zhang, X., Wang, H., Liu, G., Wang, G., Zhang, H. and Zhao, H. (2018). One-step synthesis of cobalt-doped MoS_2 nanosheets as bifunctional electrocatalysts for overall water splitting under both acidic and alkaline conditions. *Chemical Communication, 54,* 3859-3862.

Xie J., Zhang, J., Li, S., Grote, F., Zhang, X., Zhang, H., Wang, R., Lei, Y., Pan, B. and Xie, Y. (2013). Controllable disorder engineering in oxygen-incorporated MoS_2 ultrathin nanosheets for efficient hydrogen evolution. *Journal of American Chemical Society,135(47),* 17881–17888.

Xu, S., Lei, Z. and Wu, P. (2015). Facile preparation of 3D $MoS_2/MoSe_2$ nanosheet–graphene networks as efficient electrocatalysts for the hydrogen evolution reaction. *Journal of Material Chemistry A,3,* 16337.

Yang, Y., Fei, H., Ruan, G., Li, Y., Tour, J.M. (2015). Vertically aligned WS_2 nanosheets for water splitting. *Advanced Functional Materials, 25,* 6199-6204.

Yang, L., Fu, Q., Wang, W., Huang, J., Huang, J., Zhang, J. and Xiang,B. (2015). Large-area synthesis of monolayer $MoS_{2(1-x)}Se_{2x}$ with a tunable band gap and its enhanced electrochemical catalytic activity. *Nanoscale,7,* 10490.

Ye, G., Gong, Y., Lin, J., Li, B., He, Y., Pantelides, S. T., Zhou, W., Vajtai, R. and Ajayan, P. M. (2016). Defects engineered monolayer $MoS_2$for improved hydrogen evolution reaction. *Nano Letters, 16*, 1097.

Yin, M., Wang, K., Zhang, L., Gao, C., Ren, J. and Yu, L. (2023). Ternary alloyed MoS2–x Se x nanocomposites with a carrier mobility-dominated gas sensing mode: a superior room temperature gas sensing material for NO_2 sensors. *Journal of Materials Chemistry C, 11*, 9715–9726.

Yin, Y., Han, J., Zhang, Y., Zhang, X., Xu, P., Yuan, Q., Samad, L., Wang, X., Wang, Y., Zhang, Z., Zhang, P., Cao, X., Song, B. and Jin, S. (2016). Contributions of phase, sulfur vacancies and edges to the hydrogen evolution reaction catalytic activity of porous molybdenum disulfide nanosheets. *Journal of American Chemical Society,138 (25),* 7965-7972. https://doi.org/10.1021/jacs.6b03714.

Yin, Y., Zhang, Y., Gao, T., Yao, T., Zhang, X., Han, J., Wang, X., Zhang, Z., Xu, P., Zhang, P., Cao X., Song, B. and Jin, S. (2017). Synergistic Phase and Disorder Engineering in 1T-$MoSe_2$ Nanosheets for Enhanced Hydrogen-Evolution Reaction. *Advanced Materials, 29(28),* 1700311. https://doi.org/10.1002/adma.201700311.

Yu, T. and Breslin, C.B. (2020). Review-two-dimensional titanium carbide MXenes and their emerging applications as electrochemical sensors. *Jounal of Electrochemical Society, 167*, 037514.

Yu, P., Wang, F., Shifa, T. A., Zhan, X., Lou, X., Xia, F. and He, J. (2019). Earth abundant materials beyond transition metal dichalcogenides: A focus on electrocatalyzing hydrogen evolution reaction. *Nano Energy, 58*, 244-276.

Yu, J., Peng, G., Peng, L., Chen, Q., Su, C., Shang, L. and Zhang, T. (2024). Recent advancements in two-dimensional transition metal dichalcogenide materials towards hydrogen-evolution electrocatalysis, *Green Energy & Environment*, https://doi.org/10.1016/j.gee.2024.08.009.

Zeng, J. Liu, Y., Huang, Z., Qiao, H. and Qi, X. (2024). Transition metal dichalcogenides in electrocatalytic water splitting. *Catalysts, 14*, 689. https://doi.org/10.3390/catal14100689.

Zhang, L., Chang, Q., Chen, H. and Shao, M. (2016). Recent advances in palladium-based electrocatalysts for fuel cell reactions and hydrogen evolution reaction. *Nano Energy, 29*,198–219.

Zhang, K., Kim H.-J., Lee, J.-T., Chang, G.-W., Shi, X., Kim, W., Ma, M., Kong, K.-j., Choi, J.-M., Song, M.-S. and Park, J.H. (2014). Unconventional pore and defect generation in molybdenum disulfide: Application in high-rate lithium-ion batteries and the hydrogen evolution reaction. *ChemSusChem, 7*, 2489-2495.

Zhang, X., Meng, F., Mao, S., Ding, Q., Shearer, M. J., Faber, M. S., Chen, L., Hamers, R. J. and Jin, S. (2015). Amorphous MoSxCly electrocatalyst supported by vertical graphene for efficient electrochemical and photoelectrochemical hydrogen generation. *Energy and Environmental Science, 8,* 862-868.

Zhang, K. et al., (2020). Enhancement of van der Waals interlayer coupling through polar Janus MoSSe. *Journal of American Chemical Society, 142*, 17499.

Zhang, Y, Liu, K, Wang, F, Shifa, T.A, Wen, Y, Wang, F., et al. (2017). Dendritic growth of monolayer ternary $WS_{2(1-x)}Se_{2x}$ flakes for enhanced hydrogen evolution reaction, 9, 5641–5647.

Zhao, C., Liu, B., Piao S, Wang X, Lobell DB, Huang Y, Huang M et al., (2017). Temperature increase reduces global yields of major crops in four independent estimates. *Prococeeding of National Academy of Science, USA, 114(35),* 9326-9331. https://doi.org/10.1073/pnas.1701762114.

Zhou, P., Li, N., Chao, Y., Zhang, W., Lv, F., Wang K., Yang, W., Gao, P. and Guo, S. (2019). Thermolysis of noble metal nanoparticles into electron-rich phosphorus-coordinated noble metal single atoms at low temperature. *Angew Chem Int Ed Engl., 58(40),* 14184-14188. https://doi.org/10.1002/anie.201908351.

Zhu, J., Hu, L., Zhao, P., Lee, L. Y. S. and Wong, K.-Y. (2020). Recent advances in electrocatalytic hydrogen evolution using nanoparticles. *Chemical Review, 120*, 851.

Zhu, Z.Y., Cheng ,Y.C. and Schwingenschlögl, U. (2011). Giant spin-orbit-induced spin splitting in two-dimensional transition-metal dichalcogenide semiconductors. *Physical Review B: Condensed Matter,84*, 153402.

Zibouche N., Kuc A., Musfeldt, J. and Heine, T. (2014). Transition-metal dichalcogenides for spintronic applications. *Annalen der physik, 526* , 395-401